Global organisation of structural covariance networks derived from parcellated cortical surface area in atypical populations

William Roseby[1], Chris Racey[1] and Jamie Ward[1]

[1]School of Psychology, University of Sussex

Abstract

Higher-order features of brain organisation are powerful measures for understanding the relationship between brain and experience. In particular, the global arrangement of structural features of the cortex provides insight into neurodevelopmental processes that underlie individual differences in perception and cognition. Structural covariance networks (SCNs), which capture regional coordination of brain morphometry, are an efficient method to derive global properties of the cortex. However, their interpretation relies on an array of methodological choices that are often inconsistent between studies. Using a hierarchically-clustered version of the Human Connectome Project (HCP) atlas, we constructed SCNs of regional cortical surface area for groups with four different conditions – synaesthesia, autism, early psychosis, and anxiety or depression – and compared global network properties with those of age- and sex-matched controls. SCNs for synaesthesia and autism showed globally stronger connectivity, with specific increases at moderate cortical distances, as well as lower network complexity. Conversely, the SCN for early psychosis showed a globally lower connectivity and a greater complexity, while depression and anxiety showed few differences compared to controls. The results for autism and depression were replicated across two datasets each. These findings support the notion that synaesthesia and autism share neurodevelopmental mechanisms, while psychosis may involve a diverging process. This study is also an important proof of principle for analysing diverse populations under one methodological framework.

1 Introduction

A driving question in cognitive neuroscience is how the organisation of the brain is related to differences in perception, cognition, emotion, and overall experience. One method of characterising brain organisation is to examine the properties of cortical networks, where nodes represent specific regions of cortex and connections reflect the degree of association between them. This data-driven approach contrasts the examination of specific regions in isolation, which can improve statistical power but also introduce bias and constrain the hypothesis space (Wilson et al., 2024). The construction of global networks serves as a form of dimensionality reduction, rendering interpretable the higher-order properties of the brain which may be more sensitive to perturbation and more important for high-level cognitive processes (Montembeault et al., 2012; King et al., 2021; Vetter et al., 2025). Therefore, they may be particularly primed to uncover neural organisational principles that are strongly related to experiential qualities (Mišić and Sporns, 2016; Tompson et al., 2018).

Structural covariance networks (SCNs) are networks computed using structural MRI data by deriving the correlations between the morphometrics of different brain regions. Being based on structural features like grey matter volume, cortical thickness, or cortical surface area, these correlations capture the degree of coordinated growth of different regions that is driven by neurodevelopmental processes (Mechelli et al., 2005; Zielinski et al., 2010; Alexander-Bloch, Giedd and Bullmore, 2013). However, this structural association has also been shown to reflect genetic influences (Schmitt et al., 2008), experience-dependent plasticity and aging (Draganski et al., 2004; Montembeault et al., 2012), as well as white matter connectivity (Gong et al., 2012; Moura et al., 2017) and functional connectivity (Bhojraj et al., 2010; Alexander-Bloch, Raznahan, Bullmore and Giedd, 2013; Geerligs et al., 2016). Therefore, structural covariance presents a general yet powerful measure for cortical association and connectivity. Indeed, SCN topology has been used successfully to predict the status of various conditions like Alzheimer's, Parkinson's and schizophrenia (Diao et al., 2024; Mongay-Ochoa et al., 2025; Vetter et al., 2025). This power of this approach is augmented by its methodological advantages, which include the wider availability, lower computational cost, and greater signal-to-noise ratio of structural MRI compared to functional and diffusion MRI (Bethlehem et al., 2017; Diao et al., 2024). However, SCN studies on some conditions like autism have shown conflicting results (Bethlehem et al., 2017; Cai et al., 2021; Wang et al., 2022), which is likely

attributable to methodological choices such as the structural measure, cortical parcellation scheme, correlation metric, and the application of thresholding, binarisation, or selection of positive or negative correlations (Liang et al., 2009; Zalesky et al., 2010; Joshi et al., 2010; Gong et al., 2012; Geerligs et al., 2016; Carmon et al., 2020). Therefore, there is a need to examine a variety of phenotypes following the same analysis pipeline.

The application of a consistent methodological framework across various cognitive phenotypes also bears important conceptual implications. Atypical cognitive phenotypes, such as autism, synaesthesia, psychosis, and depression, can serve as models to understand the relationship between brain organisation and experience. Yet, addressing how these diverse phenotypes are related through neurodevelopmental pathways may inherently require a comparative approach (Ward, 2021). Bayesian brain and predictive processing accounts have offered a unifying conceptual framework for each of these conditions, with changes to the relative balance of prior predictions and sensory information proposed to underlie an assortment of cognitive features (Adams et al., 2013; Lawson et al., 2014; Seth, 2014; Van de Cruys et al., 2017; Sterzer et al., 2018; Friston, 2020). Importantly, some have proposed a diametrical model of autism and psychosis, positing they lie at opposite ends of a single continuum (Crespi and Badcock, 2008; Rządeczka et al., 2023). However, how these theoretical alterations to inference relate to brain organisation is unclear, limiting the strength of conclusions regarding their neurodevelopmental overlap. Yet, some empirical evidence already reveals patterns between these atypical experiences. For example, autistic populations have higher rates of synaesthesia (Baron-Cohen et al., 2013; Hughes et al., 2017), a phenomenon where a perception of one kind induces a percept in a different sensory modality. Those with synaesthesia also report higher levels of autistic traits (Ward et al., 2017; van Leeuwen et al., 2019), and there is evidence for a genetic association of synaesthesia with autism, but not with schizophrenia (Nugent and Ward, 2022). Interestingly, autism and psychotic disorders also co-occur at an elevated rate, but whether this reflects troublesome diagnosis is unclear (Zhou et al., 2019; Trevisan et al., 2020), and evidence for a genetic overlap is inconclusive (Chandrasekhar et al., 2020; Jutla et al., 2022). Neurobiological findings of cortical networks tend to diverge, with autism showing greater between-network and short-range connectivity particularly involving the default mode network (DMN) (Müller et al., 2011; Hong et al., 2019; Ilioska et al., 2023; Weber et al., 2024; Lee et al., 2025), and psychosis / schizophrenia showing a pattern of increased connectivity within and between the DMN, salience network

(SN) and fronto-parietal network (FPN) (Whitfield-Gabrieli et al., 2009; Hare et al., 2019; Del Fabro et al., 2021; Menon et al., 2023). A consistent finding is that autism, synaesthesia and psychosis are all associated with elevated rates of depression and anxiety (Achim et al., 2011; Hollocks et al., 2019; Li et al., 2020; Neufeld et al., 2025). However, while the former are all highly heritable (Bosley and Eagleman, 2015; Tick et al., 2016; Hilker et al., 2018), depression and anxiety are shaped more strongly by life circumstances, making it difficult to disentangle neurodevelopmental influences from societal and environmental factors like stigmatisation. A comparative approach may also be uniquely beneficial in this respect.

In this study, we used SCNs to examine the global structural organisation of the brain across a variety of atypical conditions including synaesthesia, autism, early psychosis, depression and anxiety, which were individually compared with age- and sex-matched controls. SCNs were constructed using cortical surface surface area from the Human Connectome Project (HCP) atlas parcellation, which was first clustered to generate a smaller set of 62 contiguous cortical regions. Edge weights in the SCNs were then calculated as the group-wise partial correlations between surface area values. Surface area was used because it has been shown to be substantially more robust for SCN pipelines than other measures (Carmon et al., 2020). Parcellated surface area is also less studied than cortical thickness, but these features may have distinct genetic influences (Panizzon et al., 2009; van der Meer et al., 2020) and surface area likely better reflect the group differences seen in synaesthesia and autism (Hazlett et al., 2017; Ward et al., 2024). Similarly, we used partial correlations over standard pearson correlations because they better represent pairwise relationships and have shown to align more closely with structural connectivity (Wheland et al., 2012; Masuda et al., 2018). In addition to comparing abstract network topology, the role of physical organisation was also analysed by aligning network weights with cortical distances. In agreement with some prior studies on cortical thickness (Hänggi et al., 2011; Wang et al., 2022), we found increased structural correlation in surface area for synaesthesia and autism groups compared to controls. Contrastingly, there was evidence for globally decreased structural correlation in early psychosis, and no group differences in anxiety and depression samples, supporting the notion that structural correlations more strongly reflect neurodevelopmental processes. The results were consistent across several datasets where they were available, suggesting robustness of the analysis.

2 Methods

The study methods were pre-registered on OSF following preliminary findings with the Syn100 dataset (https://osf.io/xzwav/overview). In addition to examining the present atypical populations, we originally planned to incorporate network comparisons across ages and between sexes. For brevity we exclude them here. We also restricted our analysis to surface area rather than cortical thickness. We do not include our analysis on the local clustering coefficient as it provided little additional insight over the global measure. Otherwise, our analyses conform to the pre-registrated methods. We expanded on network complexity as one of our stated exploratory analyses.

2.1 Data collection

No primary data collection occurred in this study. Seven specific datasets were accessed for secondary analysis. These included: synaesthesia 100 brains (Syn100) (Racey et al., 2023), the Autism Brain Imaging Data Exchange (ABIDE)-I (Di Martino et al., 2014), ABIDE-II (Di Martino et al., 2017), the Human Connectome Project for Early Psychosis (HCP-EP) (Prunier and Shenton Martha; Breier, n.d.), the Boston Adolescent Neuroimaging of Depression and Anxiety (BANDA) (Hubbard et al., 2024), Dimensional Connectomics of Anxious Misery (DCAM), and Perturbation of the Treatment of Resistant Depression Connectome by Fast-Acting Therapies (PDC). Some data were also acquired from the HCP Development/Aging (HCP-DA) (Harms et al., 2018) and HCP Young Adult (HCP-YA) (Van Essen et al., 2013) cohorts for supplementing numbers of healthy controls.

The Syn100 dataset was already available to us from a previous study (Racey et al., 2023). ABIDE-I and ABIDE-II data were downloaded from the Neuroimaging Tools & Resources Collaboratory (NITRC) amazon web service (aws) S3 bucket, located at s3://fcp-indi/data/Projects/ABIDE and s3://fcp-indi/data/Projects/ABIDE2 respectively. HCP-EP, BANDA, DCAM, PDC, and HCP-D were downloaded from the NIMH data archive (NDA). HCP-YA data were downloaded from the ConnectomeDB aws S3 bucket, located at s3://hcp-openaccess/HCP1200/. Collected data included T1w MRI scans in .nii.gz format, HCP preprocessed structural data, and phenotypic data including age, sex, and condition status. In the case of PDC, only pre-treatment data were collected.

2.2 Statement of ethics

As stated in the original study (Ward et al., 2024), participants in the Syn100 dataset gave informed consent for both participation and data sharing and the project was approved by the Brighton and Sussex Medical School (BSMS) Research Governance and Ethics Committee. Data from the NDA was accessed for research purposes following the Data Use Certification with approval from the NDA Data Access Committee. Data from the Neuroimaging Tools & Resources Collaboratory (NITRC) was accessed following registration. See Acknowledgements for further details on accessing each dataset.

2.3 Participant selection

Sample	Age (mean years +/- SD)	Sex (% female)	Data sources
Syn100	Control: 35.34 (+/-13.15) Aff: 35.38 (+/-13.20)	Control: 78.43 Aff: 77.45	Control: UoS, HCP-YA, HCP-DA Aff: UoS
ABIDE-I	Control: 29.95 (+/-7.14) Aff: 30.82 (+/-8.73)	Control: 17.65 Aff: 16.67	Control: ABIDE-I Aff: ABIDE-I
ABIDE-II	Control: 28.65 (+/-11.17) Aff: 28.37 (+/-11.44)	Control: 13.73 Aff: 13.73	Control: ABIDE-II Aff: ABIDE-II
HCP-EP	Control: 23.28 (+/-3.92) Aff: 23.40 (+/-3.59)	Control: 53.92 Aff: 46.08	Control: HCP-EP, HCP-YA, HCP-DA Aff: HCP-EP
BANDA	Control: 15.43 (+/-1.07) Aff: 15.66 (+/-0.87)	Control: 70.59 Aff: 77.45	Control: BANDA, HCP-DA Aff: BANDA
DCAM	Control: 30.54 (+/-9.67) Aff: 30.82 (+/-8.88)	Control: 75.49 Aff: 76.47	Control: DCAM, HCP-YA, HCP-DA Aff: DCAM
PDC	Control: 34.10 (+/-10.72) Aff: 36.59 (+/-12.73)	Control: 74.51 Aff: 77.45	Control: PDC, HCP-YA, HCP-DA Aff: PDC

Table 1: Demographics and data sources for control and affected groups for each dataset. UoS = University of Sussex.

The sample size for the smallest dataset was $N = 102$ participants in the synaesthete group. In order to facilitate comparable analyses, we constrained every dataset to this same sample size. Some additional criteria were placed on certain datasets: 18+ years of age in ABIDE, and for the BANDA participants with anxiety and depression were placed into a single group termed Mood Disorder (MD).

Participants were selected via a 1:1 optimal matching procedure by sex and age in most

cases. The 'affected' group (with a positive diagnosis or assessment) were first selected by matching to the synaesthete sample; BANDA was matched according to sex only. The control group were then selected via matching the affected group of $N = 102$ to available control participants. The control pool for the Syn100 dataset was the same as the original study, which was $N = 650$ participants comprising a mixture of HCP-YA and HCP-DA subjects, as well as some participants scanned at the University of Sussex (Ward et al., 2024). For HCP-EP, BANDA, DCAM and PDC, there were insufficient internal control participants for a 1:1 matching. In these cases, all internal controls were used and the remaining affected group were matched to HCP-YA and HCP-DA participants. Participants were never used twice across datasets. This matching procedure produced groups of $N = 102$ for all datasets, with very close age and sex distributions for each paired control and affected groups. There was not more than a year between mean ages, and $< 7\%$ difference in sex proportions in the worst case (Table 1).

A power analysis for comparison of $n = 1891$ network correlations suggested that a $\beta = 0.8$ ($\alpha = .05$) would be sufficient to detect a difference in means of $d = 0.091$ and a difference in variances of $f = 0.046$. A simplified version of a permutation test suggested that for a comparison of means from two sets of $n = 102$ observations, each drawn randomly from a normal distribution, the estimated power is approximately 0.8 ($\alpha = .05$) for a difference in distribution means of $d = 0.4$. Therefore, our analysis appeared moderately well-powered to detect medium effect sizes, although this could differ for derived measures that do not follow a normal distribution.

2.4 MRI preprocessing and feature extraction

Preprocessing of structural data differed depending on whether the data were raw T1w scans (ABIDE-I, ABIDE-II, HCP-EP, DCAM) or were already preprocessed with the HCP pipeline (Syn100, BANDA, PDC). The HCP preprocessing pipeline is a multi-step process which parcellates each subject's cortex into 180 anatomically and functionally segregated regions per hemisphere. This first step involves the preprocessing and alignment of T1w and T2w scans, leveraging FreeSurfer to generate surface meshes. The pipeline then implements an algorithm called multimodal surface matching (MSM), in which a pre-trained classifer is applied to T1w, T2w, and fMRI scans to extract and fit the cortical surface to the 360 region

HCP parcellation scheme (Glasser et al., 2016). In the case of HCP preprocessed datasets, the parcellation algorithm had already been run and the parcellated regions were extracted using connectome workbench.

However, not all datasets had undergone the HCP preprocessing pipeline, which is computationally expensive to run for large sample sizes and requires multimodal images that were not available for all datasets. For these datasets, we instead aligned images to the HCP atlas using T1w data alone. T1w scans were first preprocessed using FreeSurfer (version 7.4.1, (Fischl, 2012)) *recon-all* to obtain the cortical meshes. The Glasser atlas in fsaverage space was then applied to each subject's surface mesh. The resulting atlas was then used to parcellate the freesurfer meshes. Absolute surface area (in mm^2) for a parcel was calculated as the area sum over all vertices in the parcel. All surface mapping and parcellation steps were carried out in MATLAB version 9.7.0.1339299 R2019B.

Within each dataset, scans were sometimes acquired from different sites which can impact absolute structural measurements (Hedges et al., 2022). Therefore, ComBat harmonization was applied to the surface area values of dataset using the neuroCombat R package (Fortin, 2025). Scan site, which also encompassed preprocessing in those cases with participant differences, was used as the batch variable, while sex, age, and group of interest were included as covariates.

2.5 Structural covariance network construction

Surface area values for the 360 HCP parcels werefirst reduced to 180 values by taking the mean across hemispheres. SCNs are often defined using inter-regional Pearson correlations (Alexander-Bloch, Giedd and Bullmore, 2013); however, the weights of specific edges can be confounded by indirect relationships through other vertices (Masuda et al., 2018). Therefore, partial correlations were used instead, which regress out the effects of other vertices on specific pairwise relationships and have also been shown to better reflect structural connectivity (Joshi et al., 2010). This constructs a network in which each edge weight represents the unique shared variance in surface area between two regions.

Solving the partial correlation matrix via covariance matrix inversion was not possible due to rank deficiency ($102 < 180$). Instead of regularization methods, we opted for dimensionality

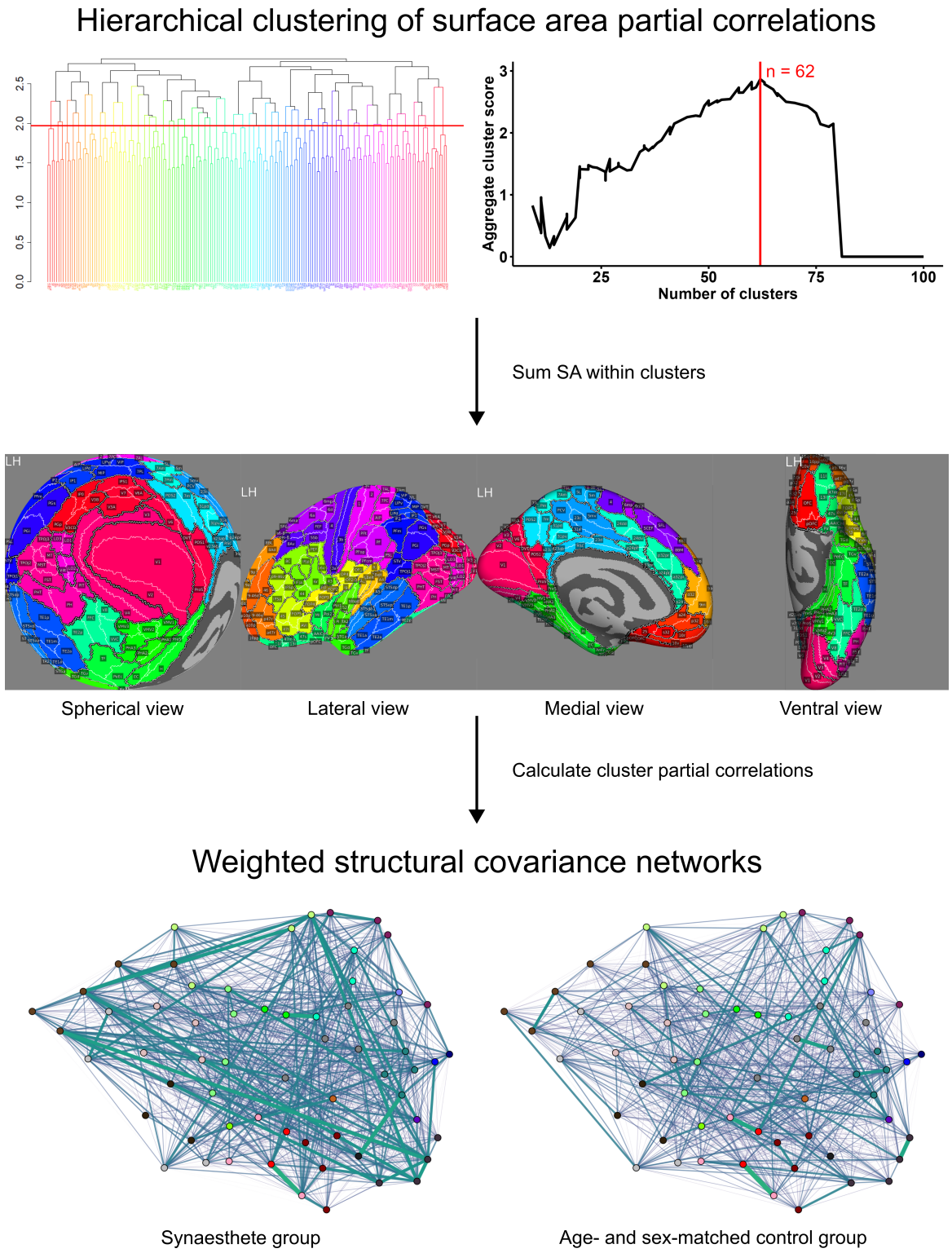

Figure 1: Process of constructing per-sample structural covariance networks (SCNs). Partial correlations between HCP parcel surface areas were calculated for a group of healthy controls ($N = 650$), which underwent hierarchichal clustering to generate 62 clusters of neighbouring parcels. Partial correlations between clusters were used generate SCNs for each control and affected group. In the SCN diagrams, line thickness and opacity reflects the magnitude of the partial correlation between two clusters.

reduction via hierarchical clustering (HC). To capture parcel dependencies, the HC algorithm, using Ward's criterion (Ward, 1963), was run on the partial correlation matrix estimated from a sample of $N = 650$ healthy controls used in a prior study (Ward et al., 2024). To identify a set of robust clusters, numbers of clusters ranging from 9 to 100 were assessed for quality and consistency. Separation and compactness of clusters was measured using mean silhouette score and the Dunn index. Consistency of the clustering was measured using the adjusted Rand index, which was assessed for separate clusterings of data from the left and right hemispheres, as was as for clusterings from 20 random subsamples of $N = 325$ from the full $N = 650$ control group. These metrics were normalised and summed into a single score. To ensure the selected clustering was not due to biased random sampling, the process was repeated 10 times using 10 random seeds. This process suggested 62 clusters 8/10 times, and 57 clusters 2/10 times, so 62 clusters was selected as optimal. Clusters contained a range of 2-5 parcels, with a mean of 2.90. Intruigingly, 100% of clusters were comprised entirely of parcels that share borders. This finding suggests that neighbouring regions of the cortex share similar profiles of surface area relationships with the rest of the cortex. This is not to suggest that proximal regions necessarily have similar morphology, but that they expand or contract in a coordinated fashion with respect to the rest of the cortical surface.

Surface area values for each group were summed across parcels belonging to the same cluster. The partial correlation matrix $\tilde{R}$ of the cluster SA values was estimated for each group via inversion of the covariance matrix Σ. To ensure partial correlations adequately captured the dependency structure of the clusters, cluster surface areas were statistically checked for normality using the Anderson-Darling test, as well as for differences in variance between compared groups using the F-test. Within each sample, the proportion of normally-distributed clusters was generally high, ranging from $60\% - 90\%$, while the variance differences were zero or very low in most cases (Supplementary Material Table S1), suggesting that partial correlations were able to capture the majority of the dependence structure between the clusters. Graphs $G(V, E)$ representing SCNs were created from the partial correlation matrices using the graph-tool python package (version 2.79, Peixoto (2017)), where the clusters defined vertices v_i (with $i = 1, \ldots, n$, and with $n = 62$) and the absolute partial correlation magnitudes $|\rho_{ij}^{\text{partial}}|$ defined edge weights w_{ij} from vertex v_i to vertex v_j. Weight thresholds were not applied, meaning SCNs were fully connected in the first instance. However, two subnetworks containing only positive or negative correlations were also analysed for each group.

2.6 Network metric calculations

Weighted network metrics including the global clustering coefficient, characteristic path length, global efficiency, and betweenness centrality were calculated using graph-tool. For path length, efficiency and betweenness centrality, edge weights were inverted prior to the calculation, as edge weights reflect association rather than cost. Global clustering C, which reflects the degree of organisation of network weights into triangles, is calculated according to Zhang and Horvath (2005) as:

$$C = \frac{TrA^3}{\sum_{i \neq j} [A^2]_{ij}}$$

Where A is the connectivity matrix, in this case equal to the absolute partial correlation matrix $|\tilde{R}|$. Characteristic path length L, representing the average shortest distance between vertices, was calculated as:

$$L = \frac{1}{N(N-1)} \sum_{i \neq j} d_{ij},$$

where each direct connection A_{ij} is treated as having length $1/A_{ij}$ and d_{ij} is the shortest-path distance between vertices v_i and v_j computed from these lengths. Similarly, global efficiency E_{glob}, which reflects the ease of communication across the network, was calculated as:

$$E_{\text{glob}} = \frac{1}{N(N-1)} \sum_{i \neq j} \frac{1}{d_{ij}}.$$

Betweenness centrality C_B, which represents how many of the shortest paths travel via a given vertex v_i, was calculated as:

$$C_B(v_i) = \sum_{\substack{v_j, v_k \in V \\ j \neq k \\ j \neq i \\ k \neq i}} \frac{\sigma_{jk}(v_i)}{\sigma_{jk}},$$

where σ_{jk} is the number of shortest paths from the source vertex v_j to target vertex v_k and $\sigma_{jk}(v_i)$ is the number of shortest paths from v_j to v_k that pass through vertex v_i. The values were normalised by the numbers of pairs of vertices not including v_i.

Edge weight diversity was also investigated as a means of indexing network complexity. Jensen–Shannon (JS) divergence was used to capture heterogeneity in the patterns of edge weights between vertices, as this compares two probability distributions for their dissimilarity (Bai and Hancock, 2012). Distributions of edge weights w for each vertex v_i to all vertices $\{v_1, \ldots, v_n\}$ were first normalised to create a probability vector p_i. For each specific target vertex v_j:

$$p_i(j) = \begin{cases} \dfrac{w_{ij}}{\sum_{k=1}^{n} w_{ik}}, & \text{if } \sum_{k=1}^{n} w_{ik} > 0, \\ \dfrac{1}{n}, & \text{otherwise,} \end{cases} \qquad j = 1, \ldots, n.$$

For any two vertices v_i and v_j, let

$$m_{ij}(k) = \tfrac{1}{2}\big(p_i(k) + p_j(k)\big).$$

The prerequisite to JS divergence is the Kullback–Leibler (KL) divergence, which from from p_i to m_{ij} is calculated as:

$$D_{\mathrm{KL}}\big(p_i \| m_{ij}\big) = \sum_{k=1}^{n} p_i(k)\ \log_2 \frac{p_i(k)}{m_{ij}(k)}.$$

The JS divergence (JSD) between the edge weight distributions of vertices i and j is the symmetric version of the KL divergence and was calculated as:

$$\mathrm{JSD}_{ij} = \tfrac{1}{2} D_{\mathrm{KL}}\big(p_i \| m_{ij}\big) + \tfrac{1}{2} D_{\mathrm{KL}}\big(p_j \| m_{ij}\big)$$

which satisfies $\mathrm{JSD}_{ij} = \mathrm{JSD}_{ji}$ and $\mathrm{JSD}_{ii} = 0$.

To establish the average divergence of one vertex v_i, we took the mean of JS divergences of vertex v_i to all vertices:

$$\mathrm{JSD}_i = \frac{1}{n} \sum_{j=1}^{n} \mathrm{JSD}_{ij} \, .$$

Finally, to establish a single JS divergence value for a network ($\mathrm{JSD}_{\mathrm{global}}$), we took the mean JS divergence between all pairs of vertices:

$$\mathrm{JSD}_{\mathrm{global}} = \frac{1}{n^2} \sum_{i=1}^{n} \sum_{j=1}^{n} \mathrm{JSD}_{ij} = \frac{2}{n^2} \sum_{1 \leq i < j \leq n} \mathrm{JSD}_{ij},$$

where the second equality uses the symmetry $\mathrm{JSD}_{ij} = \mathrm{JSD}_{ji}$ and $\mathrm{JSD}_{ii} = 0$.

In summary, $\mathrm{JSD}_{\mathrm{global}}$ quantifies, in bits, the mean JS divergence between all pairs of edge weight distributions in the weighted network.

2.7 Cortical geodesic and small-world propensity calculations

Anatomically relevant distances between parcel clusters were estimated by calculating geodesics on the spherical cortical surface. Cluster centres were calculated as the 3-dimensional centroids of fsaverage vertices belonging to each cluster. This can be problematic in some cases when non-uniform region shapes lead to the centre of mass being outside the region itself. Therefore cluster centres were checked visually, and in all cases the centroids were located inside the clusters as the majority of clusters were roughly circular. The geodesic between centre points $\mathbf{P}$ of clusters i and j was calculated as:

$$r \cdot \mathrm{atan2}\left(\left\|\mathbf{P}_i \times \mathbf{P}_j\right\|, \mathbf{P}_i \cdot \mathbf{P}_j\right)$$

Where r is the sphere radius. The calculation was repeated for all pairwise combinations of clusters to obtain cortical distances associated with every cluster correlation.

Small-world propensity (SWP) was calculated as in Muldoon et al. (2016), using cortical distances between clusters as derived above. Empirical networks were reconfigured into two null models: a lattice network where the largest edge weights are at the shortest distances, and an ensemble of 10 random networks where edge weights were shuffled randomly. SWP ϕ was then calculated as a function of the observed and null global clustering coefficients and characteristic path lengths:

$$\phi = 1 - \sqrt{\frac{\Delta_C^2 + \Delta_L^2}{2}}$$

where

$$\Delta_C = \frac{C_{latt} - C_{obs}}{C_{latt} - C_{rand}}$$

$$\Delta_L = \frac{L_{obs} - L_{rand}}{L_{latt} - L_{rand}}$$

Delta δ, which represents the extent to which the divergence from perfect small-worldness ($\phi = 1$) is due to a too lattice-like or too random-like topology, was calculated also as:

$$\delta = \frac{4\alpha}{\pi} - 1$$

where

$$\alpha = \tan^{-1}(\frac{\Delta_L}{\Delta_C})$$

A delta close to -1 therefore relfects an observed network with a clustering coefficient maximally different to its lattice null model, while a delta close to +1 reflects an observed network with a path length maximally different to its random null model.

2.8 Statistical analysis

Statistical analysis was carried in R (version 4.5.0, R Core Team (2025)) and python (version 3.1.0). Normality tested was performed using the Shapiro-Wilk test or the Anderson-Darling test. Group comparisons of distribution means and variances for normal distributions (e.g., partial correlations) were implemented with Welch's t-test and F-tests repsectively. FDR correction was used in the case of sets of multiple tests.

Group comparisons of descriptive statistics for non-normal distributions (e.g., betweenness centrality) were implemented using permutation tests with 10,000 iterations. One-sided P-values were then calculated as the proportion of times the null group differences were more extreme than the observed group difference in the chosen test direction. Group comparisons of global network properties, for which only one value per network is obtained, were also implemented using permutation tests. Here, group labels were swapped at the level of the SA data and network metrics re-calculated within each iteration for a total of 10,000 iterations. Effect sizes for differences in global metrics were calculated as the observed group difference normalised by the standard deviation of the null difference distribution. Standard error for the global metrics was estimated using jackknife (leave-one-out) resampling.

The non-linear relationship between cortical geodesic distance and network weights was modelled using Generalized Additive Models (GAMs). The mgcv R package (Wood, 2017) was used to fit Gaussian GAMs with weight as the response variable, per-group distance smooth terms and a parametric group term. This process fits a smooth weight-distance curve separately for each group, and also estimates the overall difference in weight due to group. Smooth terms were always fit with a basis dimension k of 5, chosen during preliminary testing to provide adequate flexibility without overfitting. Otherwise, parameters were left as default. Statistical significance of the parametric and smooth terms was estimated via t-tests and approximate F-tests respectively. To test for differences in the group-specific smooths, the full model was compared with a reduced model lacking group-separated smooths using a χ^2 analysis of deviance. To examine group differences along specific distances, model predictions at 100 equidistant points spanning the observed cortical distances were compared using pointwise Z-tests, applying FDR correction for multiple comparisons.

3 Results

3.1 Distributions of structural correlations

Partial correlations between cortical regions were normally distributed around zero in all cases ($P > .05$, $n = 1891$, Shapiro-Wilk test). To investigate potential differences in correlation structure between affected and control groups, we employed t-tests and F-tests. The t-tests were used to check for group differences in correlation sign, as a mean shift away from zero would indicate more positive or negative correlations on average. We found no significant differences in mean correlation, suggesting no biases towards positive or negative correlations in any condition. We then compared overall correlation magnitudes using F-tests for variances, as a change in variance would indicate correlations closer to or further from zero. These tests revealed significant increases in variance in the synaesthesia, ABIDE-I and -II datasets, as well as a significant decrease in the HCP-EP dataset (Table 2). This indicates that the synaesthesia and autism networks possessed greater magnitude correlations, while the early psychosis network had generally weaker correlations. Visual examination of the distributions suggested these effects applied for both positive and negative directions (Figure 2).

Sample	**t-test** $t_{(3740.8)}$	**t-test P-value**	**F-test** $F_{(1890,1890)}$	**F-test P-value**
Syn100	0.06	.9489	0.79	$<$ **.0001**
ABIDE-I	-0.03	.9768	0.84	**.0001**
ABIDE-II	0.03	.9745	0.84	**.0001**
HCP-EP	0.03	.9778	1.10	**.0330**
BANDA	0.03	.9780	0.97	.4517
DCAM	0.01	.9910	0.96	.4007
PDC	0.01	.9894	0.98	.6780

Table 2: Tests for group differences in partial correlation distributions. $n = 1891$ for all tests.

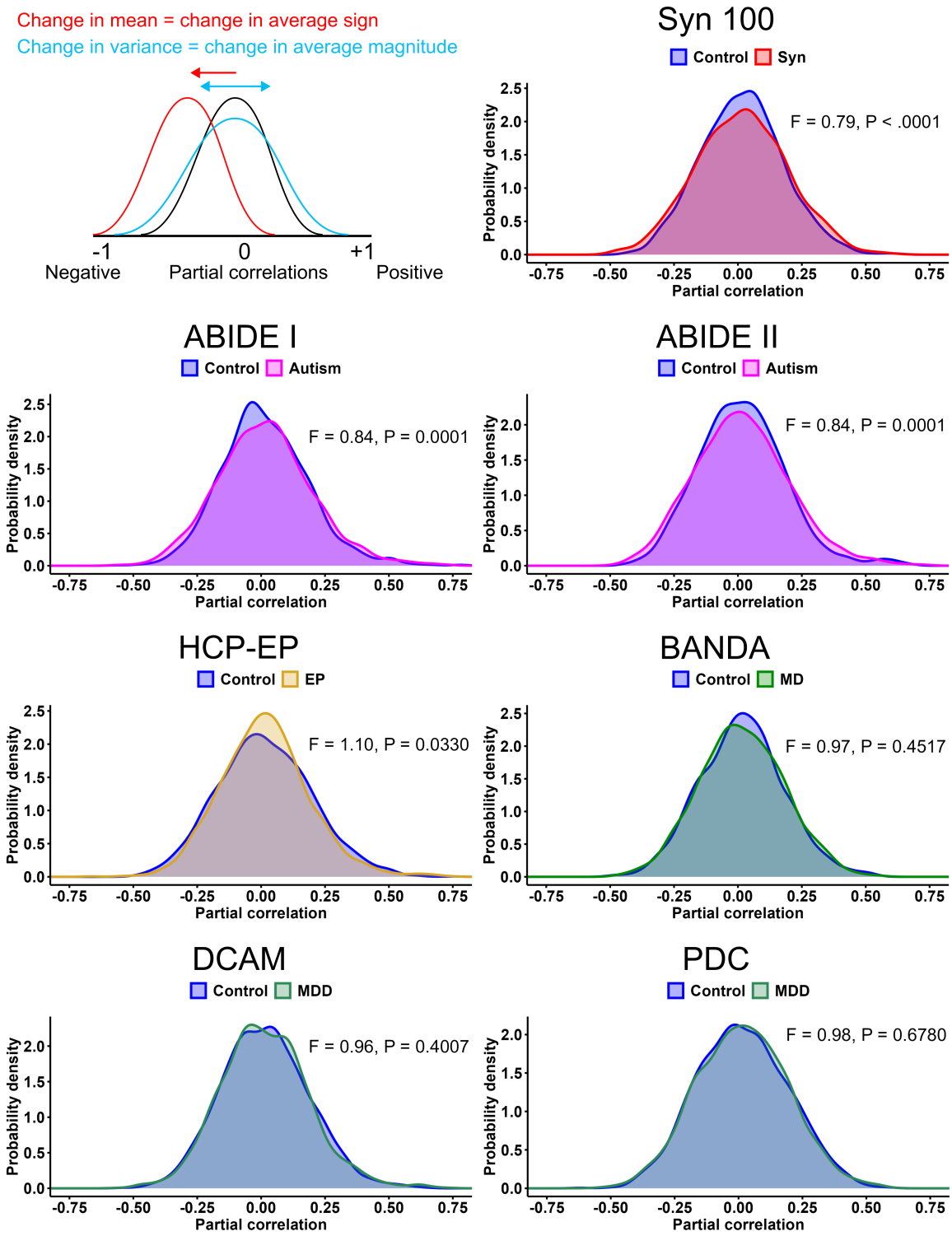

Figure 2: Distributions of partial correlations for control and affected groups in each dataset. Changes in mean would reflect changes in average sign, while changes in variance would reflect changes in average correlation magnitude. F-values pertain to F-tests for variance, $n = 1891$ observations.

3.2 SCN network properties

For the global network metrics, we hypothesised that synaesthesia and autism networks would display increased clustering and efficiency and reduced path length, in accordance with previous research using cortical thickness (Hänggi et al., 2011). In the synaesthesia network, a statistically significant decrease in path length was observed, while efficiency and clustering coefficient showed numerical but non-significant increases ($P = .103$). In ABIDE-I and ABIDE-II, the same pattern was observed, with some non-significant changes with the strongest effect for decreased path length in ABIDE-II. Following the diametric model (Crespi and Badcock, 2008), we hypothesised that HCP-EP would show opposing effects to autism and synaesthesia. However, while there were numerical decreases in efficiency and clustering, and an increase in path length, these were not statistically significant. In BANDA, DCAM and PDC, the same pattern as in synaesthesia and autism was observed, but there was no statistical significance (Figure 3, Table 3). The pattern of effect sizes follows the pattern of statistical significance, with relatively large effect sizes for the synaesthesia and ABIDE samples and smaller effects in the other samples. To check if these results were specific to the clustering scheme, the analysis for the Syn100 dataset was re-run across six adjustments to the number of clusters. The same patterns were observed for both the partial correlation distributions and network metrics (Supplementary Material Table S2), demonstrating these results were robust to region selection. Similar results were also observed in SCNs formed from positive or negative correlations only, with path length showing significant decreases in synaesthesia ($P = .033$) but non-significant decreases in autism ($P = .059$, Supplementary Material Tables S3 and S4). Overall, these results suggest that network topology in surface area SCNs may be best distinguished by characteristic path length. They also suggest that synaesthesia and autism possess similar network changes compared to controls.

The distribution of centrality values across vertices can also provide insight into the hierarchical organisation of the network. All samples displayed a centrality distribution characterised by many vertices with low centrality and decreasing numbers of vertices with higher centrality. In line with research on functional connectivity (Hong et al., 2019; Ward et al., 2024), we hypothesised that synaesthesia and autism networks would show compressed hierarchies compared to their controls, as indicated by flatter distributions of centrality values. However, except for a small increase in variance in synaesthesia, comparison of distribution shape revealed no group differences in any datasets (Figure 4). The small effects observed here

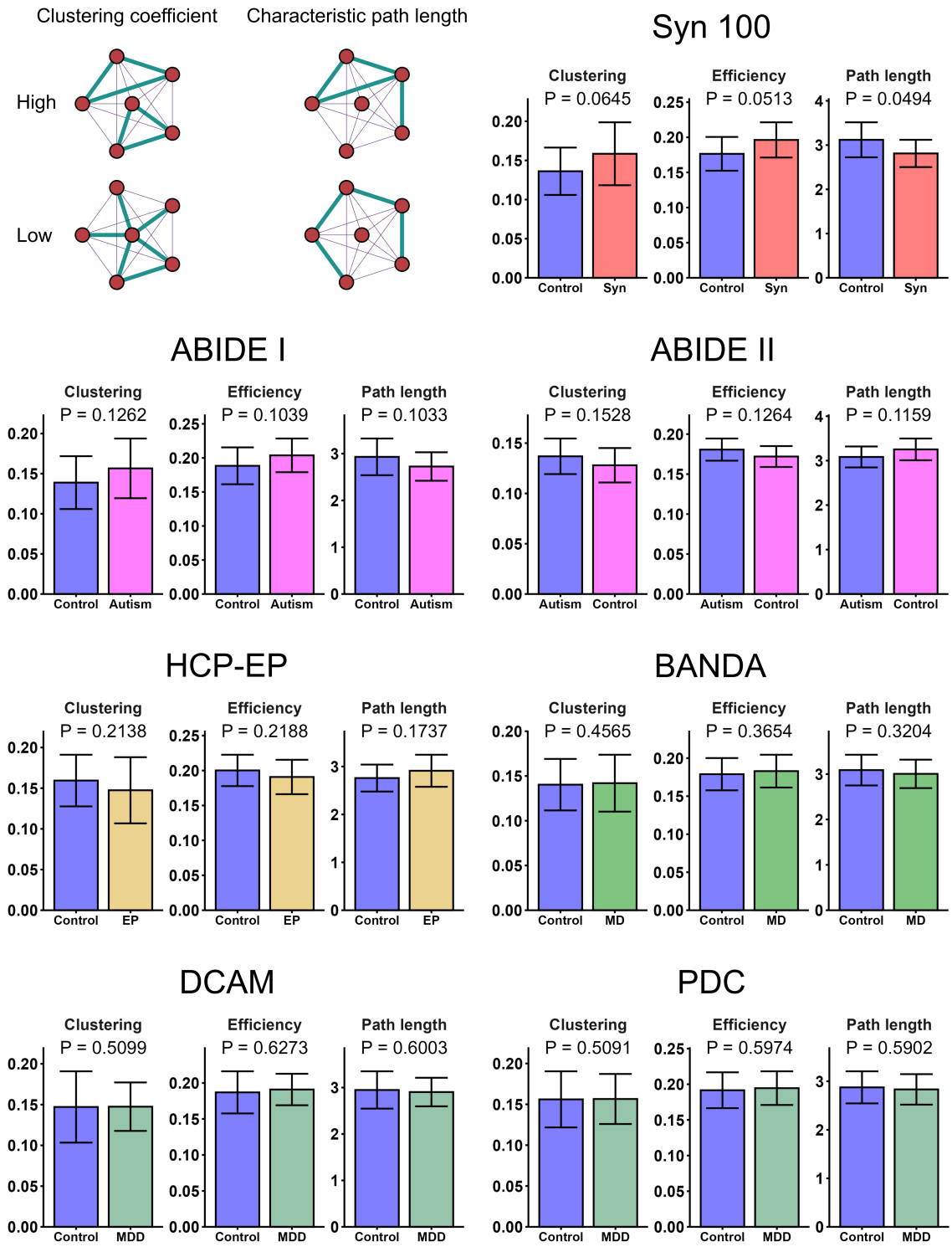

Figure 3: Global network metrics of SCNs. The diagram in the top left shows toy networks with high and low clustering and path length, whereby the thicker lines represent larger edge weights. P-values were calculated via permutation tests with $10,000$ permutations, while standard error was estimated through jackknife resampling.

Sample	Clustering	Clustering effect size	Clustering P-value	Global efficiency	Global efficiency effect size	Global efficiency P-value	Path length	Path length effect size	Path length P-value
Syn100	Control: 0.136 Aff: 0.158	1.49	.0645	Control: 0.176 Aff: 0.196	1.64	.0513	Control: 3.119 Aff: 2.810	-1.67	**.0494**
ABIDE-I	Control: 0.139 Aff: 0.157	1.08	.1262	Control: 0.188 Aff: 0.204	1.24	.1039	Control: 2.932 Aff: 2.725	-1.26	.1033
ABIDE-II	Control: 0.128 Aff: 0.137	0.99	.1528	Control: 0.172 Aff: 0.181	1.14	.1264	Control: 3.253 Aff: 3.083	-1.2	.1159
HCP-EP	Control: 0.159 Aff: 0.147	-0.75	.2138	Control: 0.200 Aff: 0.191	-0.76	.2188	Control: 2.759 Aff: 2.911	0.94	.1737
BANDA	Control: 0.140 Aff: 0.142	0.1	.4565	Control: 0.179 Aff: 0.183	0.34	.3654	Control: 3.088 Aff: 3.005	-0.46	.3204
DCAM	Control: 0.147 Aff: 0.147	0.01	.5099	Control: 0.187 Aff: 0.191	0.31	.6273	Control: 2.948 Aff: 2.904	-0.25	.6003
PDC	Control: 0.156 Aff: 0.157	0.03	.5091	Control: 0.192 Aff: 0.195	0.25	.5974	Control: 2.875 Aff: 2.833	-0.23	.5902

Table 3: Group differences in global network metrics of SCNs. P-values were calculated via permutation tests with $n = 10000$ permutations. Effect size for each measure is analogous to Cohen's d, calculated using the observed group difference in metrics normalised by the null (shuffled) distribution standard deviation

suggest that none of these conditions are associated with a departure of the structural network from the typical hierarchical organisation characterised by many low-importance regions and fewer high-importance regions. Similar results were observed in positive- and negative-only networks (Supplementary Material Tables S5 and S6). Furthermore, across samples, mean group differences in correlation strength showed no clear differences between known functional connectivity networks (Yeo et al., 2011), suggesting global structural changes were also not predominantly localised within specific functional regions (Supplementary Material Table S7).

Network complexity was assessed using Jensen–Shannon divergence between the edge weight distributions of all vertices. Significant decreases in mean JS divergence were observed in synaesthesia, ABIDE-I and -II, and BANDA samples, as well as a significant increase in the HCP-EP sample, the latter showing the largest effect size (Table 4). This suggests that synaesthesia, autism and adolescent anxiety SCNs have decreased complexity, while the early psychosis SCN bears substantially increased complexity. These differences could further reflect the globally increased cortical interactivity in synaesthesia and autism, leading to more homogeneous associations between regions, while the reduced interactivity in early psychosis reflects regions with more specialised associations.

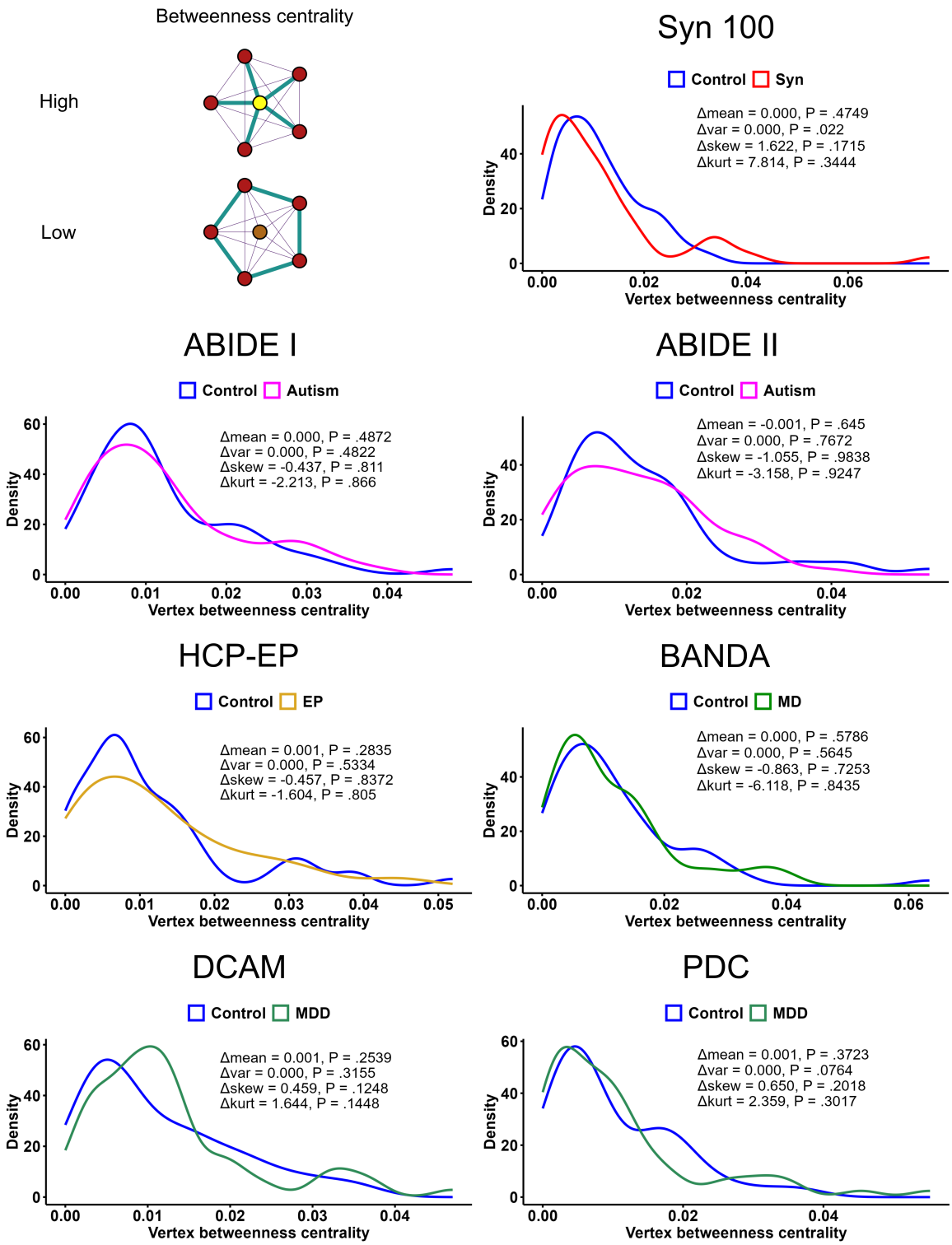

Figure 4: Distributions of betweenness centrality values. The diagram shows toy networks where the central vertex has high and low betweenness centrality. For each dataset, betweenness values were compared between affected and control groups in terms of their Pearson correlation, means, variance, skewness and kurtosis. P-values were estimated via permutation tests for $10,000$ permutations, $n = 62$ observations.

Sample	SW normal P-value	$t_{(118.25)}$	Cohen's d	P-value
Syn100	Control: **.0266** Aff: .7069	2.97	-0.53	**.0036**
ABIDE-I	Control: .5126 Aff: .6599	3.02	-0.54	**.0031**
ABIDE-II	Control: .8317 Aff: .6362	2.69	-0.48	**.0081**
HCP-EP	Control: .7472 Aff: .8204	-6.65	1.19	$<$ **.0001**
BANDA	Control: .2410 Aff: .9722	2.14	-0.38	**.0342**
DCAM	Control: .2560 Aff: **.0166**	-1.81	0.32	.0732
PDC	Control: .4174 Aff: .0526	0.48	-0.09	.6331

Table 4: Group differences in mean Jensen-Shannon divergence of edge weight distributions. $n = 62$ observations. SW = Shapiro-Wilk.

3.3 Spatial organisation of network weights

To assess if changes in network weights followed a spatial pattern, we modelled the relationship between weight and cortical distance using generalized additive models (GAMs). We hypothesised that autism and synaesthesia would have stronger weights at longer distances over the cortex, in line with structural and functional connectivity findings in autism (Müller et al., 2011; Weber et al., 2024). All samples displayed a highly significant smooth term for distance (Table 5), indicating that distance has a consistently non-linear relationship with network weights. This relationship was characterized by strong weights at short distances that quickly flattened to consistent yet lower weight at longer distances (Figure 5), suggesting that like other brain networks, SCNs possess the strongest weights at short distances. In no case was a significant interaction between group and the smooth distance term observed (Table 5), suggesting that the conditions analysed do not deviate from this regular pattern. Significant effects of group were observed for the synaesthesia, ABIDE-I and -II and HCP-EP datasets, but not for the DCAM, PDC or BANDA datasets (Table 5). This provides further

Sample	Group coefficient	Group coefficient SE	Group coefficient $t_{(3772.363)}$	Group coefficient P-value	Smooth term F	Smooth term P-value	Group:smooth deviance	Group:smooth P-value
Syn100	0.016	0.003	4.918	$<$ **.0001**	Control: 24.21 Aff: 25.34	Control: $<$ **.0001** Aff: $<$ **.0001**	0.032	.5289
ABIDE-I	0.013	0.003	3.836	**.0001**	Control: 75.12 Aff: 84.43	Control: $<$ **.0001** Aff: $<$ **.0001**	0.061	.2295
ABIDE-II	0.014	0.003	4.037	$<$ **.0001**	Control: 91.32 Aff: 70.56	Control: $<$ **.0001** Aff: $<$ **.0001**	0.045	.3791
HCP-EP	-0.011	0.003	-3.312	**.0009**	Control: 57.10 Aff: 63.99	Control: $<$ **.0001** Aff: $<$ **.0001**	0.038	.4857
BANDA	0.004	0.003	1.147	.2515	Control: 25.86 Aff: 18.70	Control: $<$ **.0001** Aff: $<$ **.0001**	0.038	.4051
DCAM	0.000	0.003	0.144	.8855	Control: 41.17 Aff: 57.88	Control: $<$ **.0001** Aff: $<$ **.0001**	0.061	.2032
PDC	0.001	0.003	0.219	.8267	Control: 19.76 Aff: 14.88	Control: $<$ **.0001** Aff: $<$ **.0001**	0.049	.3242

Table 5: Generalised additive models (GAM) predicting network weight as a function of a parametric Group term and separate smooth Distance terms for each group. Estimated and reference degrees of freedom for F values can be found in Supplementary Material Table S10. $n = 1891$ observations per group.

support for the hypothesis that synaesthesia, autism and early psychosis show differences in global correlation strength, but that anxiety and depression groups have overall similar correlation magnitudes to healthy controls.

When comparing differences in weight between affected and control groups across varying distances, significant differences were observed for the Syn100, ABIDE-I and ABIDE-II networks, which all had increased correlation strength at moderate distances (Figure 5). Therefore it appeared that in addition to globally increased correlation strength, synaesthesia and autism were further characterised by specific increases at moderately long cortical distances compared to controls. In contrast, early psychosis showed no significant differences at specific cortical distances, suggesting a more distributed decrease in correlation strength. Somewhat similar results were observed in SCNs with positive- or negative-only correlations. Interestingly however, only positive SCNs showed the non-linear relationship between distance and weight, while negative SCNs showed no clear relationship (Supplementary Material Tables S9 and S10). Furthermore, synaesthesia showed significant weight differences at moderate- and very-long distances in the positive network, but also differences at short-to-moderate distances in the negative network; in contrast, autism showed significant differences at moderate distances in the negative network only (Supplementary Material Figures S1 and S2).

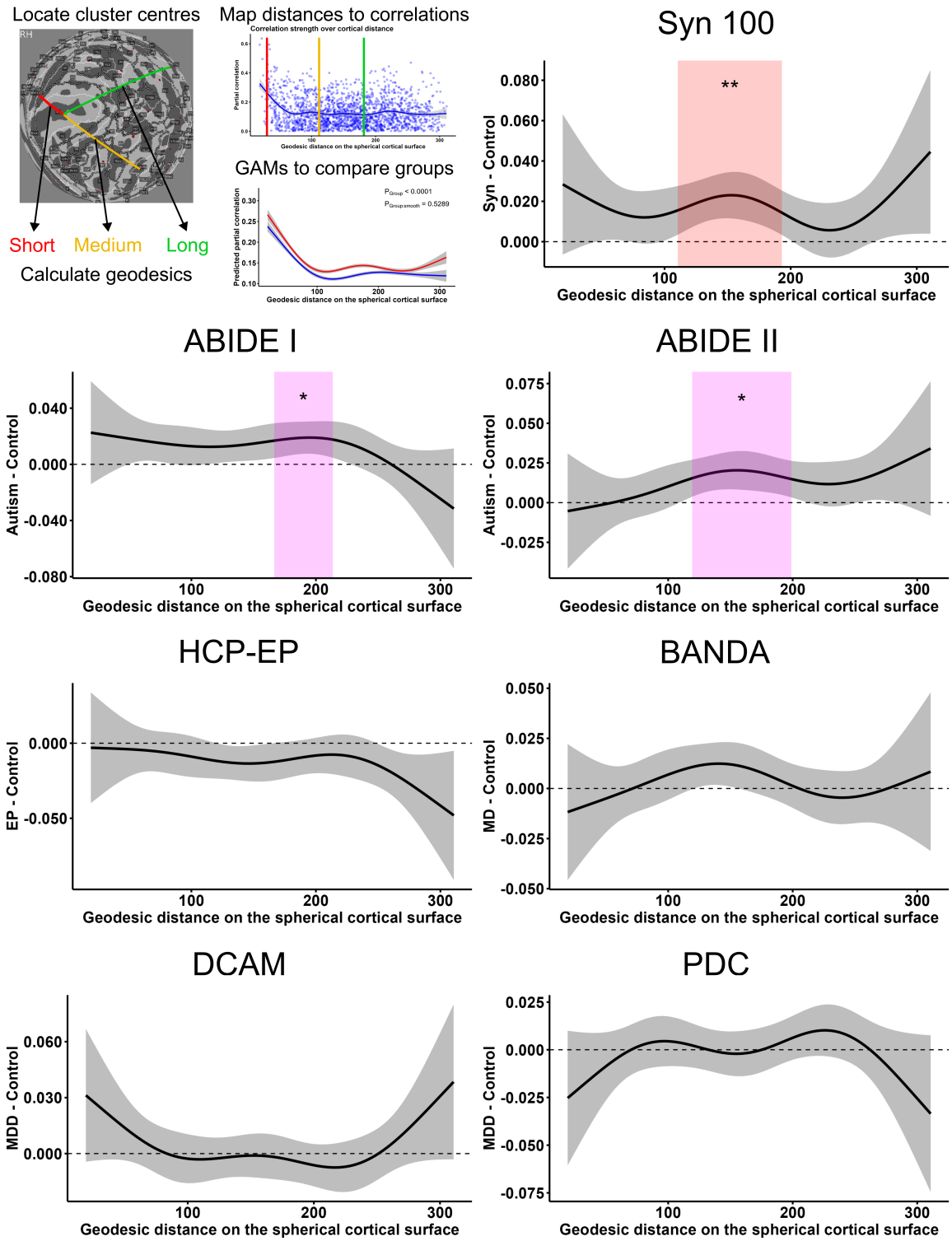

Figure 5: Group differences in network weights over the range of inter-cluster cortical distances. GAMs were used used to model the smooth relationship between cortical distance and network weight, according to group. The plots for each dataset show the group difference in predicted network weights across the range of cortical distances, with the shaded area indicating the 95% confidence interval. Distances with significant group differences are highlighted; '**' = $P < .01$, '*' = $P < .05$, with FDR correction for 100 tests. GAMs were fitted with $n = 1891$ observations per group.

Sample	SWP	delta
Syn100	Control: 0.48 Aff: 0.38	Control: -0.84 Aff: -0.69
ABIDE-I	Control: 0.57 Aff: 0.48	Control: -0.87 Aff: -0.76
ABIDE-II	Control: 0.55 Aff: 0.45	Control: -0.82 Aff: -0.76
HCP-EP	Control: 0.41 Aff: 0.44	Control: -0.73 Aff: -0.74
BANDA	Control: 0.44 Aff: 0.50	Control: -0.75 Aff: -0.80
DCAM	Control: 0.41 Aff: 0.46	Control: -0.78 Aff: -0.77
PDC	Control: 0.40 Aff: 0.41	Control: -0.67 Aff: -0.71

Table 6: Small-world propensity (SWP) and delta values of SCNs.

Spatial information was also analysed by calculating small-world propensity (SWP), which compares the observed network to lattice and random reconfigurations. Because of the computational cost of the SWP calculation, we were unable to reliably estimate statistical significance via permutation tests which were computationally unfeasible. Therefore, we report the SWP and delta measurements but make no conclusions about the robustness of any group differences. Across datasets, we observed small-world propensity (SWP) values for controls in range of 0.4-0.6 (Table 6, Figure 6), which is relatively typical if not slightly low for brain networks (Muldoon et al., 2016). In the synaesthesia and autism networks, SWP values were reduced compared to controls with an absolute difference of 0.1. Conversely, SWP was slightly increased in the HCP-EP, BANDA, DCAM and PDC datasets, although this was very small for the latter sample. This suggests that synaesthesia and autism SCNs could be characterised by reduced small-worldness. Examination of delta values, which were all close to -1, indicated that all the SCNs are characterised by very random-like topology.

Interestingly, delta values were more positive in the synaesthesia and autism networks compared to their controls, suggesting these networks were closer to a lattice configuration (i.e. strong short range connectivity) than control networks despite having reduced SWP (Ta-

ble 6,Figure 6). This apparent discrepancy is due to the fact that SWP was calculated for each SCN with reference to its own null models: therefore, synaesthesia and autism SCNs were further from both their own lattice and random null models, but slightly closer to their lattice null model compared to control networks. The decrease in SWP in synaesthesia and autism may be explained by the increases in correlation magnitudes at moderate-range distances in these networks, which confers neither local clustering nor shorter path lengths.

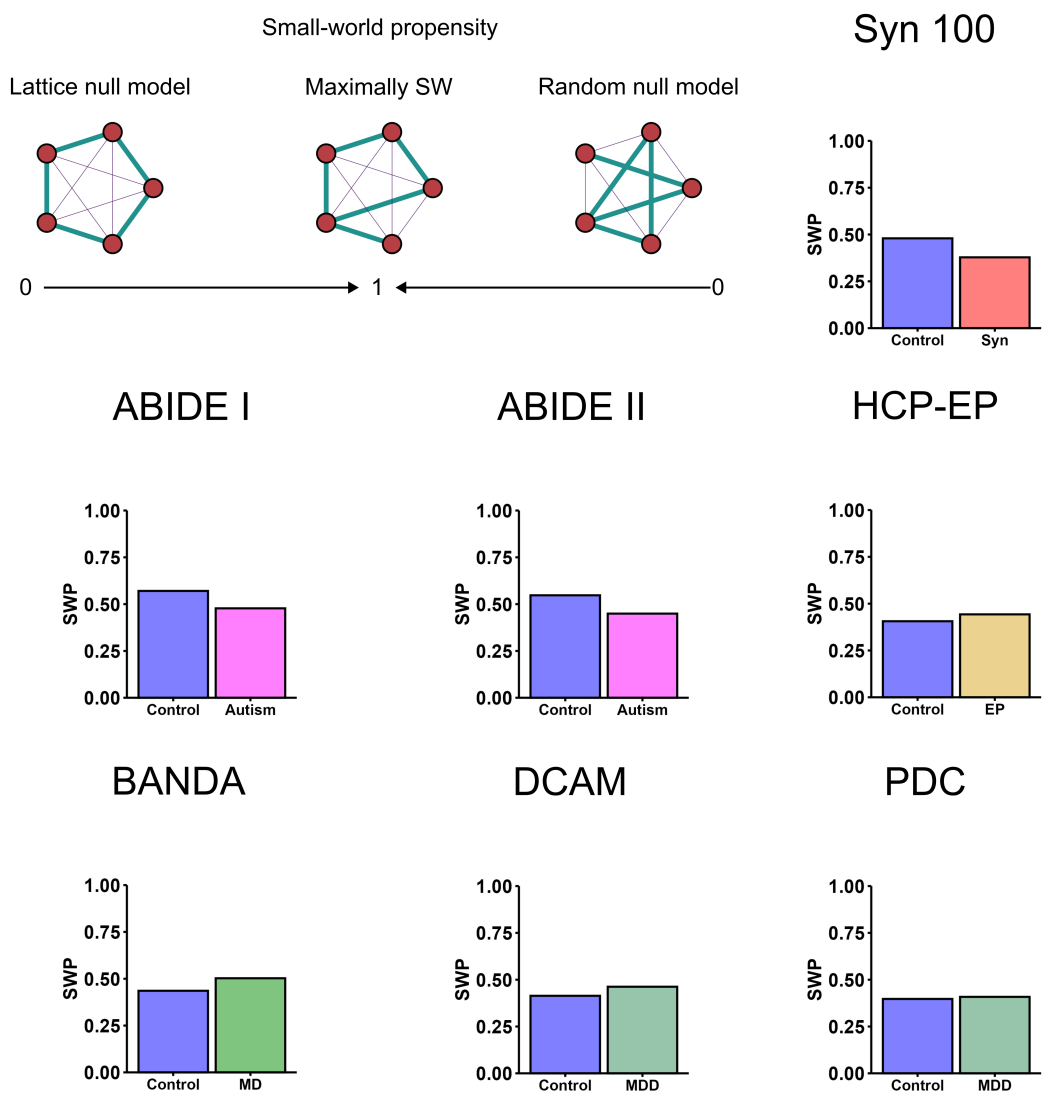

Figure 6: Small-world propensity (SWP) values. Small-worldness is largest when a network has a balance short path length, as in a random network, and high clustering coefficient, as in a lattice network. SWP was calculated by comparing the observed SCNs to null models where edge weights were randomised (random) and where the edge weights were ordered from largest to smallest over increasing cortical distance.

For positive and negative-only SCNs, findings diverged somewhat. The pattern of results was consistent in the negative SCNs, although SWP was generally lower. In contrast, all positive SCNs had the same SWP value of ~ 0.7 (Supplementary Material Table S11). This suggests that the small-world properties of SCNs is driven primarily by the positive correlations, and this is invariant across populations.

4 Discussion

The structural organisation of the brain reflects neurodevelopmental processes that underlie the coordinated maturation of distributed regions, which shapes both their specialisation and integration (Miterko et al., 2018; He et al., 2025). Structural covariance networks (SCNs) provide a window into this organisation by describing how variation in one region is linked to variation in others. This is assumed to reflect the influence of a cross-regional latent mechanism during brain development. Notably, the degree of structural covariance between two regions within a particular demographic is associated with resting-state function connectivity, white matter connectivity, and mutual genetic influences, offering insights into how regions of the cortex interact (Schmitt et al., 2008; Alexander-Bloch, Giedd and Bullmore, 2013; Alexander-Bloch, Raznahan, Bullmore and Giedd, 2013; Moura et al., 2017). However, through the assessment of global network topology, cortical SCNs also provide an opportunity to capture higher-order organisational properties like efficiency, hierarchy, small-worldness and entropy (He et al., 2009; Berlot et al., 2016; Kim et al., 2016), and these properties may be more relevant for high-level experiential traits (Mišić and Sporns, 2016; Tompson et al., 2018). By collapsing group-wide cortical organisation to single metrics, this approach can also help mitigate statistical confounds commonly present in brain-wide association studies (BWAS) that examine properties of many areas or connections (Marek et al., 2022; Burns et al., 2025). Despite this advantage, some SCN investigations of conditions like autism have failed to replicate across studies (Bethlehem et al., 2017; Cai et al., 2021; Wang et al., 2022), likely due to methodological discrepancies (Carmon et al., 2020). Thus there is a need to examine several populations under the same framework (Ward, 2021).

In this study, SCNs were leveraged to characterise the organisation of cortical surface area in several populations with atypical experiences, as compared to age- and sex-matched controls.

Hierarchical clustering of the whole-cortex HCP atlas revealed that neighbouring regions possessed similar expansion-contraction relationships with the rest of the cortex. Distributions of partial correlations beween the region clusters revealed significantly stronger associations in synaesthesia and autism, weaker correlations in early psychosis, and no change in anxiety or depression. Across SCNs using absolute, positive or negative correlations, characterisation of network topology revealed significantly lower path lengths in synaesthesia, as well as a non-significant lower path lengths in autism. Although changes in early psychosis were in the opposite direction, these were not statistically significant. Autism, synaesthesia, and adolescent anxiety networks were also characterised by significantly decreased network complexity, as measured by the divergence of edge weight distributions across vertices, while the opposite pattern was observed in early psychosis. To determine if changes in network connectivity were more prominent at specific distances, we also modelled network weights as a function of their cortical distance. Synaesthesia and autism were both characterised by increases in correlation strength at moderate distances, with diverging patterns for positive and negative correlations. Finally, the degree of small-worldness was also smaller in synaesthesia and autism networks, and slightly larger in early psychosis, anxiety and depression networks, although this was not statistically tested. The results for autism and depression were replicated across two datasets, suggesting the analysis was robust.

Our results for synaesthesia are relatively consistent with a previous study examining cortical thickness correlations in 24 grapheme-colour synaesthetes, which found decreased path length, increased global clustering, and decreased small-world properties (Hänggi et al., 2011). This is reassuring, since in addition to the different structural measure and smaller sample, this study also made disparate methodological choices including different cortical atlases, Pearson correlations, and threshold application (Hänggi et al., 2011). Therefore, the finding of increased structural network connectivity in synaesthesia appears robust. SCN studies for autism and schizophrenia or psychosis are more numerous, but also more difficult to assess; in contrast to our global approach, they have typically focussed on the covariance of *a priori* selected regions, used seed-based networks, applied strong thresholding, or employed other methodological constraints that make direct comparison unfeasible (Prasad et al., 2022). Yet, some studies have used a global approach. A study using cortical thickness correlations from autistic children saw decreased network modularity and stronger inter-module connectivity (Shi et al., 2013), which broadly aligns with our findings of decreased complexity and globally

increased correlation strength. A more recent study of cortical thickness and surface area SCNs in autistic infants also found decreased path length and increased global efficiency compared to controls, yet also decreased global clustering (Wang et al., 2022). Similarly to our approach, Bethlehem and colleagues also examined the relationship between correlation strength and cortical distance in autism using the ABIDE-I dataset. While this study found increases in correlation of surface area at moderate distances, they reported increases correlations of cortical thickness at short distances and decreases at longer distances. However, methodological details could explain this divergence: in addition to using cortical thickness rather than surface area, they measured distance as Euclidean distance between centroids (distance through the brain) while this study used geodesics (distance around the brain), and they modelled the distance-weight relationship linearly whereas we used a non-linear approach. Although they conclude a decrease in overall covariance in autism, this was only reflected in high-degree vertices (i.e., hubs) (Bethlehem et al., 2017). For psychosis and schizophrenia, studies that have examined global properties of SCNs generally agree with the current pattern of results for early psychosis, collectively finding longer path length, and lower integration, efficiency, and correlation strength in networks based on cortical thickness and white matter connectivity (Zhang et al., 2012; Griffa et al., 2015; Kim et al., 2020). Therefore, our finding of globally decreased correlation magnitude in early psychosis appears unlikely to be spurious, and perhaps reflects an early manifestation of a global schizophrenia brain phenotype. Previous results for global SCN topology in major depression have been mixed, with at least two studies finding increases in randomness reflecting a lower clustering coefficient and increased integration (Wang et al., 2016; Ping et al., 2023), and one study showing reduced global efficiency (Chen et al., 2022). Differential and null findings in depressed cohorts could reflect that the structural correlates of depression in the brain are likely to be highly individual (Han et al., 2023).

A major benefit of the current study is being able to contrast findings across these different populations. We conclude that our observed group differences cannot be due to methodological variability unlike previous studies, where groups have been studied separately with different methodological choices. Aside from population heterogeneity, another explanation for the null results in anxiety and depression is that these conditions are driven more by environmental than neurodevelopmental factors. Autism and schizophrenia are both highly heritable with a heritability around 0.7 (Tick et al., 2016; Hilker et al., 2018), and there is

evidence to suggest that synaesthesia is also highly driven by genetic factors (Bosley and Eagleman, 2015), although some evidence suggests that synaesthesia a manifestation of a broader inherited cognitive profile, i.e. a 'synaesthestic disposition' (Ward and Filiz, 2020). Although depression and anxiety are thought to have a genetic component with a heritability around 0.3 (Sullivan et al., 2000; Hettema et al., 2001), their manifestation is largely dependent on social circumstances, trauma and adversity. Thus while they are associated with structural changes such as cortical thinning (Kim et al., 2019; Schmaal et al., 2020), this may not translate to robust patterns of covariance differences. Indeed, the search for a consistent biological signature of anxiety or depression may be fundamentally flawed because these manifestations reflect individual reactions to external events rather than a genetically-driven neurodevelopmental process (Brückl et al., 2020). Thus, our results across populations are in agreement with the notion that SCNs reflect neurodevelopmental (and aging) patterns more strongly than experience-dependent plasticity or instantaneous functional connectivity (Geng et al., 2017; DuPre and Spreng, 2017).

The finding of similar global SCN changes in autism and synaesthesia aligns with the hypothesis that these conditions share a common or overlapping neurodevelopmental process (van Leeuwen et al., 2020; Nugent and Ward, 2022). In particular, globally increased connectivity, decreased complexity and lower small-worldness suggest a shift towards a more random structural organisation, a conclusion also reached by others researching autism (Ouyang et al., 2022; Wang et al., 2022). This also converges with functional studies, which indicate globally increased connectivity and contracted functional gradients, indicating increased communication between sensory and association cortices in autism (Müller et al., 2011; Hong et al., 2019; Ilioska et al., 2023; Lee et al., 2025). These converging neurobiological results may also align with theoretical predictive processing accounts of autism that suggest an increased weight on sensory information (Lawson et al., 2014; Van de Cruys et al., 2017; Friston, 2020), in that increased cortical associations could reflect a heightened tendency to pass sensory information up the cortical hierarchy. A more outstanding question is how synaesthesia and autism are differentiated, given their co-occurrence is heightened but not complete. Although we find broadly similar results for these conditions, they diverged on the role of correlation sign at different distances: synaesthesia showed greater strength positive correlations over moderate and long distances, as well as greater strength negative correlations at short-moderate distances, while autism only showed greater strength negative

correlations at moderate distance. Since positive structural correlations have been shown to reflect white matter connectivity significantly more robustly than negative correlations (Gong et al., 2012), this difference could reflect varying aspects of increased connectivity across synaesthesia and autism, which are likely to co-occur under neurodevelopmental regimes that increase connectivity more generally. Our cross-condition analysis also showed that early psychosis has reduced structural correlations as well as increased network complexity. The latter finding in particular aligns with studies showing increased hiearchical organisation in schizophrenia (Yang et al., 2023; Acero-Pousa et al., 2025), but also contrasts with studies showing greater homogeneity of connectivity (Mastrandrea et al., 2021). This current contrast between autism and psychosis finding lends itself to the diametric model of autism and psychosis, which suggests that these two conditions reflect opposing trade-offs in cognitive profile, with autism lacking mentalising ability and psychosis involving hyper-mentalising (Crespi and Badcock, 2008; Rządeczka et al., 2023). Although this model has received recent support from neurobiological findings showing disparities in EEG responses (Tarasi et al., 2022, 2023), more research is needed to test if this is also observed in global network topology.

4.1 Limitations

The study presents several important limitations. Our sample size was limited to $N = 102$, as this was the size of the smallest sample (Syn100), and we wanted to facilitate equivalent analyses across the datasets. Although this sample size is notably larger than most neuroimaging studies of synaesthesia (Racey et al., 2023), it may have lead to low statistical power across all samples in this study. Given the highly consistent patterns in network properties across datasets involving similar populations (ABIDE-I and ABIDE-II, or BANDA, DCAM and PDC), it appears more likely that lack of statistical significant differences in network metrics, particularly for autism, was driven by low statistical power rather than a true null effect. Future studies of this kind may benefit from pooling data from several samples to achieve larger sample sizes.

Relatedly, the use of hierarchical clustering to deal with the sample size being less than the number of HCP parcels (rank deficiency) also presents specific issues. On one hand, hierarchical clustering is a commonly-used approach for constructing cortical atlases or identifying networks based on voxel-wise features (Moreno-Dominguez et al., 2014; Doucet et al., 2019).

For partial correlation estimation, it is easier to interpret than commonly used regularization methods, such as graphical lasso (Friedman et al., 2008) or Ledoit-Wolf regularization (Brier et al., 2015), since it preserves empirical relationships, while the latter approaches can have unpredictable effects on the dependency structure. However, HC inherently decreases atlas resolution, which is known to affect network properties (Zalesky et al., 2010). Because the resulting networks only capture dependencies between larger areas of cortex, this could obscure certain relationships only present at smaller scales. For example, we may have seen stronger effects in autism with a higher resolution atlas, in line with other studies showing a shift to short-range connectivity in this population (Weber et al., 2024). Again, the solution to this issue lies in larger sample sizes such that atlas downsampling is not necessary. It is also important to note that for some datasets, parcellation with the HCP atlas was also carried out using T1w scans only rather than the full HCP pipeline, which uses T2w and rs-fMRI scans. This did not appear to affect results, as datasets which underwent HCP pre-processing (e.g. PDC) did not differ in correlation structure from those that did not (e.g. DCAM). However, HCP preprocessing should ideally be applied across the board for methodological consistency, which will require open datasets to either provide preprocessed data or multimodal scans.

Finally, although this study makes an important contribution in applying the same methodological pipeline to various populations, it makes no direct comparison between these populations. This is due to both lowered statistical power as well as differences in age and sex balance between the populations. Empirical support for theories like the diametric model of autism and psychosis (Crespi and Badcock, 2008) will require direct comparison of high-level neurobiological features. Dealing with this issue will require larger datasets arising from collaboration between research groups, allowing pooling of subjects such that covariates like age and sex can be appropriately balanced.

Acknowledgements

Data and/or research tools used in the preparation of this manuscript were obtained from the National Institute of Mental Health (NIMH) Data Archive (NDA). NDA is a collaborative informatics system created by the National Institutes of Health to provide a national resource

to support and accelerate research in mental health. This manuscript reflects the views of the authors and may not reflect the opinions or views of the NIH or of the Submitters submitting original data to NDA. Data were provided (in part) by the Human Connectome Project, WU-Minn Consortium (Principal Investigators: David Van Essen and Kamil Ugurbil; 1U54MH091657) funded by the 16 NIH Institutes and Centers that support the NIH Blueprint for Neuroscience Research; and by the McDonnell Center for Systems Neuroscience at Washington University. Research reported in this publication was supported by the National Institute Of Mental Health of the National Institutes of Health under Award Number U01MH109589 and by funds provided by the McDonnell Center for Systems Neuroscience at Washington University in St. Louis. The HCP-Development 2.0 Release data used in this report came from DOI: 10.15154/1520708. Research reported in this publication was supported by the National Institute On Aging of the National Institutes of Health under Award Number U01AG052564 and by funds provided by the McDonnell Center for Systems Neuroscience at Washington University in St. Louis. The HCP-Aging 2.0 Release data used in this report came from DOI: 10.15154/1520707. Research using Human Connectome Project for Early Psychosis (HCP-EP) data reported in this publication was supported by the National Institute of Mental Health of the National Institutes of Health under Award Number U01MH109977. The HCP-EP 1.1 Release data used in this report came from DOI: 10.15154/1522899. Research reported in this publication was supported by the National Institute of Mental Health under Award Number U01MH108168 to Principal Investigators John D. E. Gabrieli and Susan Whitfield-Gabrieli. The BANDA 1.1 Release data used in this report came from DOI: 10.15154/3tk5-pb47. Research reported in this publication was supported by the National Institute of Mental Health of the National Institutes of Health under Award Number U01MH109991-01. The DCAM 1.0 Release data used in this report came from DOI: 10.15154/fj45-6d13. Research reported in this publication was supported by the National Institute of Mental Health of the National Institutes of Health under Award Number U01MH110008-04. The PDC 1.0 Release data used in this report came from DOI: 10.15154/1528673 For ABIDE-I, primary support for the work by Project Coordinator Adriana Di Martino was provided by the NIMH (K23MH087770) and the Leon Levy Foundation. Primary support for the work by Michael P. Milham and the INDI team was provided by gifts from Joseph P. Healy and the Stavros Niarchos Foundation to the Child Mind Institute, as well as by an NIMH award to MPM (NIMH R03MH096321). For ABIDE-II, primary support for the work by Project Coordinator Adriana Di Martino and her team was provided by the National Institute of Mental Health (NIMH 5R21MH107045).

Primary support for the work by Michael P. Milham and his team provided by the National Institute of Mental Health (NIMH 5R21MH107045); Nathan S. Kline Institute of Psychiatric Research). Additional Support was provided by gifts from Joseph P. Healey, Phyllis Green and Randolph Cowen to the Child Mind Institute.

References

Acero-Pousa, I., Escrichs, A., Clara Dagnino, P., Sanz Perl, Y., Kringelbach, M. L., Uhlhass, P. J. and Deco, G. (2025). Reconfiguration of functional brain hierarchy in schizophrenia, *Translational Psychiatry* **15**(1): 356. doi:10.1038/s41398-025-03584-0

Achim, A. M., Maziade, M., Raymond, E., Olivier, D., Mérette, C. and Roy, M.-A. (2011). How prevalent are anxiety disorders in schizophrenia? A meta-analysis and critical review on a significant association, *Schizophrenia Bulletin* **37**(4): 811–821. doi:10.1093/schbul/sbp148

Adams, R. A., Stephan, K. E., Brown, H. R., Frith, C. D. and Friston, K. J. (2013). The computational anatomy of psychosis, *Frontiers in Psychiatry* **4**: 47. doi:10.3389/fpsyt.2013.00047

Alexander-Bloch, A., Giedd, J. N. and Bullmore, E. (2013). Imaging structural co-variance between human brain regions, *Nature Reviews Neuroscience* **14**(5): 322–336. doi:10.1038/nrn3465

Alexander-Bloch, A., Raznahan, A., Bullmore, E. and Giedd, J. (2013). The Convergence of Maturational Change and Structural Covariance in Human Cortical Networks, *The Journal of Neuroscience* **33**(7): 2889–2899. doi:10.1523/JNEUROSCI.3554-12.2013

Bai, L. and Hancock, E. R. (2012). Graph Complexity from the Jensen-Shannon Divergence, *in* G. Gimel'farb, E. Hancock, A. Imiya, A. Kuijper, M. Kudo, S. Omachi, T. Windeatt and K. Yamada (eds), *Structural, Syntactic, and Statistical Pattern Recognition*, Springer, Berlin,

Heidelberg, pp. 79–88.
doi:10.1007/978-3-642-34166-3_9

Baron-Cohen, S., Johnson, D., Asher, J., Wheelwright, S., Fisher, S. E., Gregersen, P. K. and Allison, C. (2013). Is synaesthesia more common in autism?, *Molecular Autism* **4**(1): 40.
doi:10.1186/2040-2392-4-40

Berlot, R., Metzler-Baddeley, C., Ikram, M. A., Jones, D. K. and O'Sullivan, M. J. (2016). Global Efficiency of Structural Networks Mediates Cognitive Control in Mild Cognitive Impairment, *Frontiers in Aging Neuroscience* **8**.
doi:10.3389/fnagi.2016.00292

Bethlehem, R. A. I., Romero-Garcia, R., Mak, E., Bullmore, E. T. and Baron-Cohen, S. (2017). Structural Covariance Networks in Children with Autism or ADHD, *Cerebral Cortex* **27**(8): 4267–4276.
doi:10.1093/cercor/bhx135

Bhojraj, T. S., Prasad, K. M., Eack, S. M., Francis, A. N., Montrose, D. M. and Keshavan, M. S. (2010). Do inter-regional gray-matter volumetric correlations reflect altered functional connectivity in high-risk offspring of schizophrenia patients?, *Schizophrenia Research* **118**(1): 62–68.
doi:10.1016/j.schres.2010.01.019

Bosley, H. G. and Eagleman, D. M. (2015). Synesthesia in twins: Incomplete concordance in monozygotes suggests extragenic factors, *Behavioural Brain Research* **286**: 93–96.
doi:10.1016/j.bbr.2015.02.024

Brier, M. R., Mitra, A., McCarthy, J. E., Ances, B. M. and Snyder, A. Z. (2015). Partial covariance based functional connectivity computation using Ledoit–Wolf covariance regularization, *NeuroImage* **121**: 29–38.
doi:10.1016/j.neuroimage.2015.07.039

Brückl, T. M., Spoormaker, V. I., Sämann, P. G., Brem, A.-K., Henco, L., Czamara, D., Elbau, I., Grandi, N. C., Jollans, L., Kühnel, A., Leuchs, L., Pöhlchen, D., Schneider, M., Tontsch, A., Keck, M. E., Schilbach, L., Czisch, M., Lucae, S., Erhardt, A. and Binder, E. B. (2020). The

biological classification of mental disorders (BeCOME) study: A protocol for an observational deep-phenotyping study for the identification of biological subtypes, *BMC Psychiatry* **20**(1): 213.
doi:10.1186/s12888-020-02541-z

Burns, C. D. G., Fracasso, A. and Rousselet, G. A. (2025). Bias in data-driven replicability analysis of univariate brain-wide association studies, *Scientific Reports* **15**(1): 6105.
doi:10.1038/s41598-025-89257-w

Cai, S., Wang, X., Yang, F., Chen, D. and Huang, L. (2021). Differences in Brain Structural Covariance Network Characteristics in Children and Adults With Autism Spectrum Disorder, *Autism Research: Official Journal of the International Society for Autism Research* **14**(2): 265–275.
doi:10.1002/aur.2464

Carmon, J., Heege, J., Necus, J. H., Owen, T. W., Pipa, G., Kaiser, M., Taylor, P. N. and Wang, Y. (2020). Reliability and comparability of human brain structural covariance networks, *NeuroImage* **220**: 117104.
doi:10.1016/j.neuroimage.2020.117104

Chandrasekhar, T., Copeland, J. N., Spanos, M. and Sikich, L. (2020). Autism, Psychosis, or Both? Unraveling Complex Patient Presentations, *Child and Adolescent Psychiatric Clinics of North America* **29**(1): 103–113.
doi:10.1016/j.chc.2019.08.003

Chen, C., Liu, Z., Xi, C., Tan, W., Fan, Z., Cheng, Y., Yang, J., Palaniyappan, L. and Yang, J. (2022). Multimetric structural covariance in first-episode major depressive disorder: A graph theoretical analysis, *Journal of psychiatry & neuroscience: JPN* **47**(3): E176–E185.
doi:10.1503/jpn.210204

Crespi, B. and Badcock, C. (2008). Psychosis and autism as diametrical disorders of the social brain, *The Behavioral and Brain Sciences* **31**(3): 241–261; discussion 261–320.
doi:10.1017/S0140525X08004214

Del Fabro, L., Schmidt, A., Fortea, L., Delvecchio, G., D'Agostino, A., Radua, J., Borgwardt,

S. and Brambilla, P. (2021). Functional brain network dysfunctions in subjects at high-risk for psychosis: A meta-analysis of resting-state functional connectivity, *Neuroscience & Biobehavioral Reviews* **128**: 90–101.
doi:10.1016/j.neubiorev.2021.06.020

Di Martino, A., O'Connor, D., Chen, B., Alaerts, K., Anderson, J. S., Assaf, M., Balsters, J. H., Baxter, L., Beggiato, A., Bernaerts, S., Blanken, L. M. E., Bookheimer, S. Y., Braden, B. B., Byrge, L., Castellanos, F. X., Dapretto, M., Delorme, R., Fair, D. A., Fishman, I., Fitzgerald, J., Gallagher, L., Keehn, R. J. J., Kennedy, D. P., Lainhart, J. E., Luna, B., Mostofsky, S. H., Müller, R.-A., Nebel, M. B., Nigg, J. T., O'Hearn, K., Solomon, M., Toro, R., Vaidya, C. J., Wenderoth, N., White, T., Craddock, R. C., Lord, C., Leventhal, B. and Milham, M. P. (2017). Enhancing studies of the connectome in autism using the autism brain imaging data exchange II, *Scientific Data* **4**: 170010.
doi:10.1038/sdata.2017.10

Di Martino, A., Yan, C.-G., Li, Q., Denio, E., Castellanos, F. X., Alaerts, K., Anderson, J. S., Assaf, M., Bookheimer, S. Y., Dapretto, M., Deen, B., Delmonte, S., Dinstein, I., Ertl-Wagner, B., Fair, D. A., Gallagher, L., Kennedy, D. P., Keown, C. L., Keysers, C., Lainhart, J. E., Lord, C., Luna, B., Menon, V., Minshew, N. J., Monk, C. S., Mueller, S., Müller, R.-A., Nebel, M. B., Nigg, J. T., O'Hearn, K., Pelphrey, K. A., Peltier, S. J., Rudie, J. D., Sunaert, S., Thioux, M., Tyszka, J. M., Uddin, L. Q., Verhoeven, J. S., Wenderoth, N., Wiggins, J. L., Mostofsky, S. H. and Milham, M. P. (2014). The autism brain imaging data exchange: Towards a large-scale evaluation of the intrinsic brain architecture in autism, *Molecular Psychiatry* **19**(6): 659–667.
doi:10.1038/mp.2013.78

Diao, Y., Xie, H., Wang, Y., Zhao, B., Yang, A. and Zhang, J. (2024). Individual Structural Covariance Network Predicts Long-Term Motor Improvement in Parkinson Disease with Subthalamic Nucleus Deep Brain Stimulation, *AJNR. American journal of neuroradiology* **45**(8): 1106–1115.
doi:10.3174/ajnr.A8245

Doucet, G. E., Lee, W. H. and Frangou, S. (2019). Evaluation of the spatial variability in the major resting-state networks across human brain functional atlases, *Human Brain Mapping* **40**(15): 4577–4587.

doi:10.1002/hbm.24722

Draganski, B., Gaser, C., Busch, V., Schuierer, G., Bogdahn, U. and May, A. (2004). Changes in grey matter induced by training, *Nature* **427**(6972): 311–312. doi:10.1038/427311a

DuPre, E. and Spreng, R. N. (2017). Structural covariance networks across the life span, from 6 to 94 years of age, *Network Neuroscience* **1**(3): 302–323. doi:10.1162/NETN_a_00016

Fischl, B. (2012). FreeSurfer, *NeuroImage* **62**(2): 774–781. doi:10.1016/j.neuroimage.2012.01.021

Fortin, J.-P. (2025). Jfortin1/neuroCombat_Rpackage. https://github.com/Jfortin1/neuroCombat_Rpackage

Friedman, J., Hastie, T. and Tibshirani, R. (2008). Sparse inverse covariance estimation with the graphical lasso, *Biostatistics* **9**(3): 432–441. doi:10.1093/biostatistics/kxm045

Friston, K. J. (2020). Bayesian Dysconnections, *American Journal of Psychiatry* **177**(12): 1110–1112. doi:10.1176/appi.ajp.2020.20091421

Geerligs, L., Cam-CAN and Henson, R. N. (2016). Functional connectivity and structural covariance between regions of interest can be measured more accurately using multivariate distance correlation, *NeuroImage* **135**: 16–31. doi:10.1016/j.neuroimage.2016.04.047

Geng, X., Li, G., Lu, Z., Gao, W., Wang, L., Shen, D., Zhu, H. and Gilmore, J. H. (2017). Structural and Maturational Covariance in Early Childhood Brain Development, *Cerebral Cortex* **27**(3): 1795–1807. doi:10.1093/cercor/bhw022

Glasser, M. F., Coalson, T. S., Robinson, E. C., Hacker, C. D., Harwell, J., Yacoub, E., Ugurbil,

K., Andersson, J., Beckmann, C. F., Jenkinson, M., Smith, S. M. and Van Essen, D. C. (2016). A multi-modal parcellation of human cerebral cortex, *Nature* **536**(7615): 171–178. doi:10.1038/nature18933

Gong, G., He, Y., Chen, Z. J. and Evans, A. C. (2012). Convergence and divergence of thickness correlations with diffusion connections across the human cerebral cortex, *NeuroImage* **59**(2): 1239–1248. doi:10.1016/j.neuroimage.2011.08.017

Griffa, A., Baumann, P. S., Ferrari, C., Do, K. Q., Conus, P., Thiran, J.-P. and Hagmann, P. (2015). Characterizing the connectome in schizophrenia with diffusion spectrum imaging, *Human Brain Mapping* **36**(1): 354–366. doi:10.1002/hbm.22633

Han, S., Zheng, R., Li, S., Zhou, B., Jiang, Y., Fang, K., Wei, Y., Pang, J., Li, H., Zhang, Y., Chen, Y. and Cheng, J. (2023). Resolving heterogeneity in depression using individualized structural covariance network analysis, *Psychological Medicine* **53**(11): 5312–5321. doi:10.1017/S0033291722002380

Hänggi, J., Wotruba, D. and Jäncke, L. (2011). Globally Altered Structural Brain Network Topology in Grapheme-Color Synesthesia, *Journal of Neuroscience* **31**(15): 5816–5828. doi:10.1523/JNEUROSCI.0964-10.2011

Hare, S. M., Ford, J. M., Mathalon, D. H., Damaraju, E., Bustillo, J., Belger, A., Lee, H. J., Mueller, B. A., Lim, K. O., Brown, G. G., Preda, A., van Erp, T. G. M., Potkin, S. G., Calhoun, V. D. and Turner, J. A. (2019). Salience-Default Mode Functional Network Connectivity Linked to Positive and Negative Symptoms of Schizophrenia, *Schizophrenia Bulletin* **45**(4): 892–901. doi:10.1093/schbul/sby112

Harms, M. P., Somerville, L. H., Ances, B. M., Andersson, J., Barch, D. M., Bastiani, M., Bookheimer, S. Y., Brown, T. B., Buckner, R. L., Burgess, G. C., Coalson, T. S., Chappell, M. A., Dapretto, M., Douaud, G., Fischl, B., Glasser, M. F., Greve, D. N., Hodge, C., Jamison, K. W., Jbabdi, S., Kandala, S., Li, X., Mair, R. W., Mangia, S., Marcus, D., Mascali, D., Moeller,

S., Nichols, T. E., Robinson, E. C., Salat, D. H., Smith, S. M., Sotiropoulos, S. N., Terpstra, M., Thomas, K. M., Tisdall, M. D., Ugurbil, K., van der Kouwe, A., Woods, R. P., Zöllei, L., Van Essen, D. C. and Yacoub, E. (2018). Extending the Human Connectome Project across ages: Imaging protocols for the Lifespan Development and Aging projects, *NeuroImage* **183**: 972–984.
doi:10.1016/j.neuroimage.2018.09.060

Hazlett, H. C., Gu, H., Munsell, B. C., Kim, S. H., Styner, M., Wolff, J. J., Elison, J. T., Swanson, M. R., Zhu, H., Botteron, K. N., Collins, D. L., Constantino, J. N., Dager, S. R., Estes, A. M., Evans, A. C., Fonov, V. S., Gerig, G., Kostopoulos, P., McKinstry, R. C., Pandey, J., Paterson, S., Pruett, J. R., Schultz, R. T., Shaw, D. W., Zwaigenbaum, L. and Piven, J. (2017). Early brain development in infants at high risk for autism spectrum disorder, *Nature* **542**(7641): 348–351.
doi:10.1038/nature21369

He, Y., Dagher, A., Chen, Z., Charil, A., Zijdenbos, A., Worsley, K. and Evans, A. (2009). Impaired small-world efficiency in structural cortical networks in multiple sclerosis associated with white matter lesion load, *Brain* **132**(12): 3366–3379.
doi:10.1093/brain/awp089

He, Y., Zeng, D., Li, Q., Chu, L., Dong, X., Liang, X., Sun, L., Liao, X., Zhao, T., Chen, X., Lei, T., Men, W., Wang, Y., Wang, D., Hu, M., Pan, Z., Zhang, H., Liu, N., Tan, S., Gao, J.-H., Qin, S., Tao, S., Dong, Q., He, Y. and Li, S. (2025). The multiscale brain structural re-organization that occurs from childhood to adolescence correlates with cortical morphology maturation and functional specialization, *PLOS Biology* **23**(4): e3002710.
doi:10.1371/journal.pbio.3002710

Hedges, E. P., Dimitrov, M., Zahid, U., Brito Vega, B., Si, S., Dickson, H., McGuire, P., Williams, S., Barker, G. J. and Kempton, M. J. (2022). Reliability of structural MRI measurements: The effects of scan session, head tilt, inter-scan interval, acquisition sequence, FreeSurfer version and processing stream, *NeuroImage* **246**: 118751.
doi:10.1016/j.neuroimage.2021.118751

Hettema, J. M., Neale, M. C. and Kendler, K. S. (2001). A Review and Meta-Analysis of the

Genetic Epidemiology of Anxiety Disorders, *American Journal of Psychiatry* **158**(10): 1568–1578.
doi:10.1176/appi.ajp.158.10.1568

Hilker, R., Helenius, D., Fagerlund, B., Skytthe, A., Christensen, K., Werge, T. M., Nordentoft, M. and Glenthøj, B. (2018). Heritability of Schizophrenia and Schizophrenia Spectrum Based on the Nationwide Danish Twin Register, *Biological Psychiatry* **83**(6): 492–498.
doi:10.1016/j.biopsych.2017.08.017

Hollocks, M. J., Lerh, J. W., Magiati, I., Meiser-Stedman, R. and Brugha, T. S. (2019). Anxiety and depression in adults with autism spectrum disorder: A systematic review and meta-analysis, *Psychological Medicine* **49**(4): 559–572.
doi:10.1017/S0033291718002283

Hong, S.-J., Vos de Wael, R., Bethlehem, R. A. I., Lariviere, S., Paquola, C., Valk, S. L., Milham, M. P., Di Martino, A., Margulies, D. S., Smallwood, J. and Bernhardt, B. C. (2019). Atypical functional connectome hierarchy in autism, *Nature Communications* **10**(1): 1022.
doi:10.1038/s41467-019-08944-1

Hubbard, N. A., Bauer, C. C. C., Siless, V., Auerbach, R. P., Elam, J. S., Frosch, I. R., Henin, A., Hofmann, S. G., Hodge, M. R., Jones, R., Lenzini, P., Lo, N., Park, A. T., Pizzagalli, D. A., Vaz-DeSouza, F., Gabrieli, J. D. E., Whitfield-Gabrieli, S., Yendiki, A. and Ghosh, S. S. (2024). The Human Connectome Project of adolescent anxiety and depression dataset, *Scientific Data* **11**(1): 837.
doi:10.1038/s41597-024-03629-x

Hughes, J. E. A., Simner, J., Baron-Cohen, S., Treffert, D. A. and Ward, J. (2017). Is Synaesthesia More Prevalent in Autism Spectrum Conditions? Only Where There Is Prodigious Talent, *Multisensory Research* **30**(3-5): 391–408.
doi:10.1163/22134808-00002558

Ilioska, I., Oldehinkel, M., Llera, A., Chopra, S., Looden, T., Chauvin, R., Van Rooij, D., Floris, D. L., Tillmann, J., Moessnang, C., Banaschewski, T., Holt, R. J., Loth, E., Charman, T., Murphy, D. G. M., Ecker, C., Mennes, M., Beckmann, C. F., Fornito, A. and Buitelaar, J. K.

(2023). Connectome-wide Mega-analysis Reveals Robust Patterns of Atypical Functional Connectivity in Autism, *Biological Psychiatry* **94**(1): 29–39.
doi:10.1016/j.biopsych.2022.12.018

Joshi, A. A., Joshi, S. H., Dinov, I., Shattuck, D. W., Leahy, R. M. and Toga, A. W. (2010). Anatomical structural network analysis of human brain using partial correlations of gray matter volumes, *2010 IEEE International Symposium on Biomedical Imaging: From Nano to Macro*, pp. 844–847.
doi:10.1109/ISBI.2010.5490118

Jutla, A., Foss-Feig, J. and Veenstra-VanderWeele, J. (2022). Autism spectrum disorder and schizophrenia: An updated conceptual review, *Autism Research: Official Journal of the International Society for Autism Research* **15**(3): 384–412.
doi:10.1002/aur.2659

Kim, H.-J., Shin, J.-H., Han, C. E., Kim, H. J., Na, D. L., Seo, S. W., Seong, J.-K. and Initiative, A. D. N. (2016). Using Individualized Brain Network for Analyzing Structural Covariance of the Cerebral Cortex in Alzheimer's Patients, *Frontiers in Neuroscience* **10**.
doi:10.3389/fnins.2016.00394

Kim, J. H., Suh, S.-i., Lee, H.-J., Lee, J.-h. and Lee, M.-S. (2019). Cortical and subcortical gray matter alterations in first-episode drug-naïve adolescents with major depressive disorder, *Neuroreport* **30**(17): 1172–1178.
doi:10.1097/WNR.0000000000001336

Kim, S., Kim, Y.-W., Jeon, H., Im, C.-H. and Lee, S.-H. (2020). Altered Cortical Thickness-Based Individualized Structural Covariance Networks in Patients with Schizophrenia and Bipolar Disorder, *Journal of Clinical Medicine* **9**(6): 1846.
doi:10.3390/jcm9061846

King, D. J., Seri, S., Catroppa, C., Anderson, V. A. and Wood, A. G. (2021). Structural-covariance networks identify topology-based cortical-thickness changes in children with persistent executive function impairments after traumatic brain injury, *NeuroImage* **244**: 118612.
doi:10.1016/j.neuroimage.2021.118612

Lawson, R. P., Rees, G. and Friston, K. J. (2014). An aberrant precision account of autism, *Frontiers in Human Neuroscience* **8**. doi:10.3389/fnhum.2014.00302

Lee, J.-e., Kim, S., Park, S., Choi, H., Park, B.-y. and Park, H. (2025). Atypical maturation of the functional connectome hierarchy in autism, *Molecular Autism* **16**(1): 21. doi:10.1186/s13229-025-00641-9

Li, W., Yang, Y., An, F.-R., Zhang, L., Ungvari, G. S., Jackson, T., Yuan, Z. and Xiang, Y.-T. (2020). Prevalence of comorbid depression in schizophrenia: A meta-analysis of observational studies, *Journal of Affective Disorders* **273**: 524–531. doi:10.1016/j.jad.2020.04.056

Liang, X., Wang, JH., Yan, CG., Kang, J., Yang, H., Tang, HH., Gong, QY., Wang, L., Zhu, CZ., Zang, YF. and He, Y. (2009). Different Correlation Metrics Reveal Different Topological Patterns in the Human Brain Functional Networks, *NeuroImage* **47**: S170. doi:10.1016/S1053-8119(09)71831-2

Marek, S., Tervo-Clemmens, B., Calabro, F. J., Montez, D. F., Kay, B. P., Hatoum, A. S., Donohue, M. R., Foran, W., Miller, R. L., Hendrickson, T. J., Malone, S. M., Kandala, S., Feczko, E., Miranda-Dominguez, O., Graham, A. M., Earl, E. A., Perrone, A. J., Cordova, M., Doyle, O., Moore, L. A., Conan, G. M., Uriarte, J., Snider, K., Lynch, B. J., Wilgenbusch, J. C., Pengo, T., Tam, A., Chen, J., Newbold, D. J., Zheng, A., Seider, N. A., Van, A. N., Metoki, A., Chauvin, R. J., Laumann, T. O., Greene, D. J., Petersen, S. E., Garavan, H., Thompson, W. K., Nichols, T. E., Yeo, B. T. T., Barch, D. M., Luna, B., Fair, D. A. and Dosenbach, N. U. F. (2022). Reproducible brain-wide association studies require thousands of individuals, *Nature* **603**(7902): 654–660. doi:10.1038/s41586-022-04492-9

Mastrandrea, R., Piras, F., Gabrielli, A., Banaj, N., Caldarelli, G., Spalletta, G. and Gili, T. (2021). The unbalanced reorganization of weaker functional connections induces the altered brain network topology in schizophrenia, *Scientific Reports* **11**(1): 15400. doi:10.1038/s41598-021-94825-x

Masuda, N., Sakaki, M., Ezaki, T. and Watanabe, T. (2018). Clustering Coefficients for Correlation Networks, *Frontiers in Neuroinformatics* **12**.
doi:10.3389/fninf.2018.00007

Mechelli, A., Friston, K. J., Frackowiak, R. S. and Price, C. J. (2005). Structural covariance in the human cortex, *The Journal of Neuroscience: The Official Journal of the Society for Neuroscience* **25**(36): 8303–8310.
doi:10.1523/JNEUROSCI.0357-05.2005

Menon, V., Palaniyappan, L. and Supekar, K. (2023). Integrative Brain Network and Salience Models of Psychopathology and Cognitive Dysfunction in Schizophrenia, *Biological Psychiatry* **94**(2): 108–120.
doi:10.1016/j.biopsych.2022.09.029

Mišić, B. and Sporns, O. (2016). From Regions to Connections and Networks: New Bridges between Brain and Behavior, *Current opinion in neurobiology* **40**: 1–7.
doi:10.1016/j.conb.2016.05.003

Miterko, L. N., Lackey, E. P., Heck, D. H. and Sillitoe, R. V. (2018). Shaping Diversity Into the Brain's Form and Function, *Frontiers in Neural Circuits* **12**: 83.
doi:10.3389/fncir.2018.00083

Mongay-Ochoa, N., Gonzalez-Escamilla, G., Fleischer, V., Pareto, D., Rovira, À., Sastre-Garriga, J. and Groppa, S. (2025). Structural covariance analysis for neurodegenerative and neuroinflammatory brain disorders, *Brain* **148**(9): 3072–3084.
doi:10.1093/brain/awaf151

Montembeault, M., Joubert, S., Doyon, J., Carrier, J., Gagnon, J.-F., Monchi, O., Lungu, O., Belleville, S. and Brambati, S. M. (2012). The impact of aging on gray matter structural covariance networks, *NeuroImage* **63**(2): 754–759.
doi:10.1016/j.neuroimage.2012.06.052

Moreno-Dominguez, D., Anwander, A. and Knösche, T. R. (2014). A hierarchical method for whole-brain connectivity-based parcellation, *Human Brain Mapping* **35**(10): 5000–5025.
doi:10.1002/hbm.22528

Moura, L. M., Crossley, N. A., Zugman, A., Pan, P. M., Gadelha, A., Del Aquilla, M. a. G., Picon, F. A., Anés, M., Amaro, E., de Jesus Mari, J., Miguel, E. C., Rohde, L. A., Bressan, R. A., McGuire, P., Sato, J. R. and Jackowski, A. P. (2017). Coordinated brain development: Exploring the synchrony between changes in grey and white matter during childhood maturation, *Brain Imaging and Behavior* **11**(3): 808–817. doi:10.1007/s11682-016-9555-0

Muldoon, S. F., Bridgeford, E. W. and Bassett, D. S. (2016). Small-World Propensity and Weighted Brain Networks, *Scientific Reports* **6**(1): 22057. doi:10.1038/srep22057

Müller, R.-A., Shih, P., Keehn, B., Deyoe, J. R., Leyden, K. M. and Shukla, D. K. (2011). Underconnected, but How? A Survey of Functional Connectivity MRI Studies in Autism Spectrum Disorders, *Cerebral Cortex* **21**(10): 2233–2243. doi:10.1093/cercor/bhq296

Neufeld, J., van Leeuwen, T. M., Kuja-Halkola, R., Lundström, S., Larsson, H., Lichtenstein, P., Bölte, S., Mataix-Cols, D. and Taylor, M. J. (2025). Genetic and environmental contributions to the link between synaesthesia and neurodevelopmental and psychiatric features: A twin study, *Translational Psychiatry* **15**(1): 240. doi:10.1038/s41398-025-03444-x

Nugent, M. and Ward, J. (2022). Familial aggregation of synaesthesia with autism (but not schizophrenia), *Cognitive Neuropsychiatry* **27**(5): 373–391. doi:10.1080/13546805.2022.2095897

Ouyang, M., Peng, Y., Sotardi, S., Hu, D., Zhu, T., Cheng, H. and Huang, H. (2022). Flattened Structural Network Changes and Association of Hyperconnectivity With Symptom Severity in 2–7-Year-Old Children With Autism, *Frontiers in Neuroscience* **15**. doi:10.3389/fnins.2021.757838

Panizzon, M. S., Fennema-Notestine, C., Eyler, L. T., Jernigan, T. L., Prom-Wormley, E., Neale, M., Jacobson, K., Lyons, M. J., Grant, M. D., Franz, C. E., Xian, H., Tsuang, M., Fischl, B., Seidman, L., Dale, A. and Kremen, W. S. (2009). Distinct Genetic Influences on Cortical

Surface Area and Cortical Thickness, *Cerebral Cortex (New York, NY)* **19**(11): 2728–2735. doi:10.1093/cercor/bhp026

Peixoto, T. P. (2017). The graph-tool python library, *(No Title)* .

Ping, L., Sun, S., Zhou, C., Que, J., You, Z., Xu, X., Cheng, Y. and Consortium, t. D. (2023). Altered topology of individual brain structural covariance networks in major depressive disorder, *Psychological Medicine* **53**(14): 6921–6932. doi:10.1017/S003329172300168X

Prasad, K., Rubin, J., Mitra, A., Lewis, M., Theis, N., Muldoon, B., Iyengar, S. and Cape, J. (2022). Structural covariance networks in schizophrenia: A systematic review Part II, *Schizophrenia Research* **239**: 176–191. doi:10.1016/j.schres.2021.11.036

Prunier, N. and Shenton Martha; Breier, A. (n.d.). Human Connectome Project for Early Psychosis – Release 1.1. doi:10.15154/1522899

R Core Team (2025). *R: A Language and Environment for Statistical Computing*, R Foundation for Statistical Computing, Vienna, Austria. https://www.R-project.org/

Racey, C., Kampoureli, C., Bowen-Hill, O., Bauer, M., Simpson, I., Rae, C., del Rio, M., Simner, J. and Ward, J. (2023). An Open Science MRI Database of over 100 Synaesthetic Brains and Accompanying Deep Phenotypic Information, *Scientific Data* **10**(1): 766. doi:10.1038/s41597-023-02664-4

Rządeczka, M., Wodziński, M. and Moskalewicz, M. (2023). Cognitive biases as an adaptive strategy in autism and schizophrenia spectrum: The compensation perspective on neurodiversity, *Frontiers in Psychiatry* **14**. doi:10.3389/fpsyt.2023.1291854

Schmaal, L., Pozzi, E., C. Ho, T., van Velzen, L. S., Veer, I. M., Opel, N., Van Someren, E. J. W., Han, L. K. M., Aftanas, L., Aleman, A., Baune, B. T., Berger, K., Blanken, T. F., Capitão,

L., Couvy-Duchesne, B., R. Cullen, K., Dannlowski, U., Davey, C., Erwin-Grabner, T., Evans, J., Frodl, T., Fu, C. H. Y., Godlewska, B., Gotlib, I. H., Goya-Maldonado, R., Grabe, H. J., Groenewold, N. A., Grotegerd, D., Gruber, O., Gutman, B. A., Hall, G. B., Harrison, B. J., Hatton, S. N., Hermesdorf, M., Hickie, I. B., Hilland, E., Irungu, B., Jonassen, R., Kelly, S., Kircher, T., Klimes-Dougan, B., Krug, A., Landrø, N. I., Lagopoulos, J., Leerssen, J., Li, M., Linden, D. E. J., MacMaster, F. P., M. McIntosh, A., Mehler, D. M. A., Nenadić, I., Penninx, B. W. J. H., Portella, M. J., Reneman, L., Rentería, M. E., Sacchet, M. D., G. Sämann, P., Schrantee, A., Sim, K., Soares, J. C., Stein, D. J., Tozzi, L., van Der Wee, N. J. A., van Tol, M.-J., Vermeiren, R., Vives-Gilabert, Y., Walter, H., Walter, M., Whalley, H. C., Wittfeld, K., Whittle, S., Wright, M. J., Yang, T. T., Zarate, C., Thomopoulos, S. I., Jahanshad, N., Thompson, P. M. and Veltman, D. J. (2020). ENIGMA MDD: Seven years of global neuroimaging studies of major depression through worldwide data sharing, *Translational Psychiatry* **10**(1): 172.
doi:10.1038/s41398-020-0842-6

Schmitt, J., Lenroot, R., Wallace, G., Ordaz, S., Taylor, K., Kabani, N., Greenstein, D., Lerch, J., Kendler, K., Neale, M. and Giedd, J. (2008). Identification of Genetically Mediated Cortical Networks: A Multivariate Study of Pediatric Twins and Siblings, *Cerebral Cortex* **18**(8): 1737–1747.
doi:10.1093/cercor/bhm211

Seth, A. K. (2014). A predictive processing theory of sensorimotor contingencies: Explaining the puzzle of perceptual presence and its absence in synesthesia, *Cognitive Neuroscience* **5**(2): 97–118.
doi:10.1080/17588928.2013.877880

Shi, F., Wang, L., Peng, Z., Wee, C.-Y. and Shen, D. (2013). Altered Modular Organization of Structural Cortical Networks in Children with Autism, *PLoS ONE* **8**(5).
doi:10.1371/journal.pone.0063131

Sterzer, P., Adams, R. A., Fletcher, P., Frith, C., Lawrie, S. M., Muckli, L., Petrovic, P., Uhlhaas, P., Voss, M. and Corlett, P. R. (2018). The Predictive Coding Account of Psychosis, *Biological Psychiatry* **84**(9): 634–643.
doi:10.1016/j.biopsych.2018.05.015

Sullivan, P. F., Neale, M. C. and Kendler, K. S. (2000). Genetic Epidemiology of Major Depression: Review and Meta-Analysis, *American Journal of Psychiatry* **157**(10): 1552–1562.
doi:10.1176/appi.ajp.157.10.1552

Tarasi, L., Martelli, M. E., Bortoletto, M., di Pellegrino, G. and Romei, V. (2023). Neural Signatures of Predictive Strategies Track Individuals Along the Autism-Schizophrenia Continuum, *Schizophrenia Bulletin* **49**(5): 1294–1304.
doi:10.1093/schbul/sbad105

Tarasi, L., Trajkovic, J., Diciotti, S., di Pellegrino, G., Ferri, F., Ursino, M. and Romei, V. (2022). Predictive waves in the autism-schizophrenia continuum: A novel biobehavioral model, *Neuroscience and Biobehavioral Reviews* **132**: 1–22.
doi:10.1016/j.neubiorev.2021.11.006

Tick, B., Bolton, P., Happé, F., Rutter, M. and Rijsdijk, F. (2016). Heritability of autism spectrum disorders: A meta-analysis of twin studies, *Journal of Child Psychology and Psychiatry, and Allied Disciplines* **57**(5): 585–595.
doi:10.1111/jcpp.12499

Tompson, S., Falk, E. B., Vettel, J. M. and Bassett, D. S. (2018). Network Approaches to Understand Individual Differences in Brain Connectivity: Opportunities for Personality Neuroscience, *Personality Neuroscience* **1**: e5.
doi:10.1017/pen.2018.4

Trevisan, D. A., Foss-Feig, J. H., Naples, A. J., Srihari, V., Anticevic, A. and McPartland, J. C. (2020). Autism Spectrum Disorder and Schizophrenia Are Better Differentiated by Positive Symptoms Than Negative Symptoms, *Frontiers in Psychiatry* **11**: 548.
doi:10.3389/fpsyt.2020.00548

Van de Cruys, S., Van der Hallen, R. and Wagemans, J. (2017). Disentangling signal and noise in autism spectrum disorder, *Brain and Cognition* **112**: 78–83.
doi:10.1016/j.bandc.2016.08.004

van der Meer, D., Frei, O., Kaufmann, T., Chen, C.-H., Thompson, W. K., O'Connell, K. S.,

Monereo Sánchez, J., Linden, D. E. J., Westlye, L. T., Dale, A. M. and Andreassen, O. A. (2020). Quantifying the Polygenic Architecture of the Human Cerebral Cortex: Extensive Genetic Overlap between Cortical Thickness and Surface Area, *Cerebral Cortex (New York, NY)* **30**(10): 5597–5603.
doi:10.1093/cercor/bhaa146

Van Essen, D. C., Smith, S. M., Barch, D. M., Behrens, T. E. J., Yacoub, E., Ugurbil, K. and WU-Minn HCP Consortium (2013). The WU-Minn Human Connectome Project: An overview, *NeuroImage* **80**: 62–79.
doi:10.1016/j.neuroimage.2013.05.041

van Leeuwen, T. M., Neufeld, J., Hughes, J. and Ward, J. (2020). Synaesthesia and autism: Different developmental outcomes from overlapping mechanisms?, *Cognitive Neuropsychology* **37**(7-8): 433–449.
doi:10.1080/02643294.2020.1808455

van Leeuwen, T. M., van Petersen, E., Burghoorn, F., Dingemanse, M. and van Lier, R. (2019). Autistic traits in synaesthesia: Atypical sensory sensitivity and enhanced perception of details, *Philosophical Transactions of the Royal Society of London. Series B, Biological Sciences* **374**(1787): 20190024.
doi:10.1098/rstb.2019.0024

Vetter, C. S., Bender, A., Dwyer, D. B., Montembeault, M., Ruef, A., Chisholm, K., Kambeitz-Ilankovic, L., Antonucci, L. A., Ruhrmann, S., Kambeitz, J., Rosen, M., Lichtenstein, T., Riecher-Rössler, A., Upthegrove, R., Salokangas, R. K. R., Hietala, J., Pantelis, C., Lencer, R., Meisenzahl, E., Wood, S. J., Brambilla, P., Borgwardt, S., Falkai, P., Bertolino, A., Koutsouleris, N. and Consortium, P. (2025). Exploring the predictive value of structural covariance networks for the diagnosis of schizophrenia, *Frontiers in Psychiatry* **16**.
doi:10.3389/fpsyt.2025.1570797

Wang, T., Wang, K., Qu, H., Zhou, J., Li, Q., Deng, Z., Du, X., Lv, F., Ren, G., Guo, J., Qiu, J. and Xie, P. (2016). Disorganized cortical thickness covariance network in major depressive disorder implicated by aberrant hubs in large-scale networks, *Scientific Reports* **6**(1): 27964.
doi:10.1038/srep27964

Wang, Y., Hu, D., Wu, Z., Wang, L., Huang, W. and Li, G. (2022). Developmental abnormalities of structural covariance networks of cortical thickness and surface area in autistic infants within the first 2 years, *Cerebral Cortex (New York, N.Y.: 1991)* **32**(17): 3786–3798. doi:10.1093/cercor/bhab448

Ward, J. (2021). Synaesthesia as a model system for understanding variation in the human mind and brain, *Cognitive Neuropsychology* **38**(4): 259–278. doi:10.1080/02643294.2021.1950133

Ward, J. and Filiz, G. (2020). Synaesthesia is linked to a distinctive and heritable cognitive profile, *Cortex; a Journal Devoted to the Study of the Nervous System and Behavior* **126**: 134–140. doi:10.1016/j.cortex.2020.01.002

Ward, J. H. J. (1963). Hierarchical Grouping to Optimize an Objective Function, *Journal of the American Statistical Association* **58**(301): 236–244. doi:10.1080/01621459.1963.10500845

Ward, J., Hoadley, C., Hughes, J. E. A., Smith, P., Allison, C., Baron-Cohen, S. and Simner, J. (2017). Atypical sensory sensitivity as a shared feature between synaesthesia and autism, *Scientific Reports* **7**: 41155. doi:10.1038/srep41155

Ward, J., Simner, J., Simpson, I., Rae, C., del Rio, M., Eccles, J. A. and Racey, C. (2024). Synesthesia is linked to large and extensive differences in brain structure and function as determined by whole-brain biomarkers derived from the HCP (Human Connectome Project) cortical parcellation approach, *Cerebral Cortex* **34**(11): bhae446. doi:10.1093/cercor/bhae446

Weber, C. F., Kebets, V., Benkarim, O., Lariviere, S., Wang, Y., Ngo, A., Jiang, H., Chai, X., Park, B.-y., Milham, M. P., Di Martino, A., Valk, S., Hong, S.-J. and Bernhardt, B. C. (2024). Contracted functional connectivity profiles in autism, *Molecular Autism* **15**(1): 38. doi:10.1186/s13229-024-00616-2

Wheland, D., Joshi, A., McMahon, K., Hansell, N., Martin, N., Wright, M., Thompson, P., Shat-

tuck, D. and Leahy, R. (2012). Robust identification of partial-correlation based networks with applications to cortical thickness data, *2012 9th IEEE International Symposium on Biomedical Imaging (ISBI)*, pp. 1551–1554.
doi:10.1109/ISBI.2012.6235869

Whitfield-Gabrieli, S., Thermenos, H. W., Milanovic, S., Tsuang, M. T., Faraone, S. V., McCarley, R. W., Shenton, M. E., Green, A. I., Nieto-Castanon, A., LaViolette, P., Wojcik, J., Gabrieli, J. D. E. and Seidman, L. J. (2009). Hyperactivity and hyperconnectivity of the default network in schizophrenia and in first-degree relatives of persons with schizophrenia, *Proceedings of the National Academy of Sciences* **106**(4): 1279–1284.
doi:10.1073/pnas.0809141106

Wilson, S., Cromb, D., Bonthrone, A. F., Uus, A., Price, A., Egloff, A., Van Poppel, M. P. M., Steinweg, J. K., Pushparajah, K., Simpson, J., Lloyd, D. F. A., Razavi, R., O'Muircheartaigh, J., Edwards, A. D., Hajnal, J. V., Rutherford, M. and Counsell, S. J. (2024). Structural Covariance Networks in the Fetal Brain Reveal Altered Neurodevelopment for Specific Subtypes of Congenital Heart Disease, *Journal of the American Heart Association: Cardiovascular and Cerebrovascular Disease* **13**(21): e035880.
doi:10.1161/JAHA.124.035880

Wood, S. N. (2017). *Generalized Additive Models: An Introduction with R, Second Edition*, 2 edn, Chapman and Hall/CRC, New York.
doi:10.1201/9781315370279

Yang, C., Zhang, W., Liu, J., Yao, L., Bishop, J. R., Lencer, R., Gong, Q., Yang, Z. and Lui, S. (2023). Disrupted subcortical functional connectome gradient in drug-naïve first-episode schizophrenia and the normalization effects after antipsychotic treatment, *Neuropsychopharmacology* **48**(5): 789–796.
doi:10.1038/s41386-022-01512-0

Yeo, B. T. T., Krienen, F. M., Sepulcre, J., Sabuncu, M. R., Lashkari, D., Hollinshead, M., Roffman, J. L., Smoller, J. W., Zöllei, L., Polimeni, J. R., Fischl, B., Liu, H. and Buckner, R. L. (2011). The organization of the human cerebral cortex estimated by intrinsic functional connectivity, *Journal of Neurophysiology* **106**(3): 1125–1165.

doi:10.1152/jn.00338.2011

Zalesky, A., Fornito, A., Harding, I. H., Cocchi, L., Yücel, M., Pantelis, C. and Bullmore, E. T. (2010). Whole-brain anatomical networks: Does the choice of nodes matter?, *NeuroImage* **50**(3): 970–983.
doi:10.1016/j.neuroimage.2009.12.027

Zhang, B. and Horvath, S. (2005). A general framework for weighted gene co-expression network analysis, *Statistical Applications in Genetics and Molecular Biology* **4**: Article17.
doi:10.2202/1544-6115.1128

Zhang, Y., Lin, L., Lin, C.-P., Zhou, Y., Chou, K.-H., Lo, C.-Y., Su, T.-P. and Jiang, T. (2012). Abnormal topological organization of structural brain networks in schizophrenia, *Schizophrenia Research* **141**(2): 109–118.
doi:10.1016/j.schres.2012.08.021

Zhou, H.-Y., Yang, H.-X., Gong, J.-B., Cheung, E. F. C., Gooding, D. C., Park, S. and Chan, R. C. K. (2019). Revisiting the overlap between autistic and schizotypal traits in the non-clinical population using meta-analysis and network analysis, *Schizophrenia Research* **212**: 6–14.
doi:10.1016/j.schres.2019.07.050

Zielinski, B. A., Gennatas, E. D., Zhou, J. and Seeley, W. W. (2010). Network-level structural covariance in the developing brain, *Proceedings of the National Academy of Sciences* **107**(42): 18191–18196.
doi:10.1073/pnas.1003109107